

# DESCRIPTION OF THE SCENARIO MACHINE

V.M. Lipunov<sup>1</sup>, K.A. Postnov<sup>2</sup>, M.E. Prokhorov<sup>3</sup>, A.I. Bogomazov<sup>4</sup>

Sternberg astronomical institute, Universitetskij prospect, 13, 119992, Moscow, Russia

## ABSTRACT

We present here an updated description of the ‘‘Scenario Machine’’ code. This tool is used to carry out a population synthesis of binary stars. Previous version of the description can be found at <http://xray.sai.msu.ru/~mystery//articles/review/contents.html>; see also (Lipunov et al. 1996b,c).

*Subject headings:* binaries: close — binaries: general

### 1. Basic equations and initial distributions

We use the current scenario of evolution of binary stellar systems based upon the original ideas that appeared in the papers by Paczyn’ski (1971); Tutukov & Yungelson (1973), van den Heuvel & Heise (1972) (see also review by van den Heuvel (1994)). The scenario for normal star evolution was joined with the ideas of neutron star evolution (see pioneer works by Shvartsman (1970, 1971a,b); Illarionov & Sunyaev (1975); Shakura (1975); Bisnovaty-Kogan & Komberg (1976), Lipunov & Shakura (1976), Savonije & van den Heuvel (1977)). This joint scenario has allowed to construct a two-dimensional classification of possible states of binary systems containing NS (Kornilov & Lipunov (1983a,b); Lipunov (1992)). According to this classification, we will distinguish four basic evolutionary stages for a normal star in a binary system:

- I — A main sequence (MS) star inside its Roche lobe (RL);
- II — A post-MS star inside its RL;
- III — A MS or post-MS star filling its RL; the mass is transferred onto the companion.

- IV — A helium star left behind the mass-transfer in case II and III of binary evolution; may be in the form of a hot white dwarf (for  $M \leq 2.5M_{\odot}$ ), or a non-degenerate helium star (a Wolf-Rayet-star in case of initial MS mass  $> 10M_{\odot}$ ).

The evolution of single stars can be represented as a chain of consecutive stages: I  $\rightarrow$  II  $\rightarrow$  compact remnant; the evolution of the most massive single stars probably looks like I  $\rightarrow$  II  $\rightarrow$  IV  $\rightarrow$  compact remnant. The component of a binary system can evolve like I  $\rightarrow$  II  $\rightarrow$  III  $\rightarrow$  IV  $\rightarrow$  compact remnant.

In our calculations we choose the distributions of initial binary parameters: mass of the primary zero age main sequence component (ZAMS),  $M_1$ , the binary mass ratio,  $q = M_2/M_1 < 1$ , the orbital separation  $a$ . Zero initial eccentricity is assumed.

The distribution of binaries by orbital separations can be taken from observations (Krajcheva et al. 1981; Abt 1983),

$$\begin{cases} f(\log a) = \text{const}, \\ \max(10R_{\odot}, \text{RL}[M_1]) < a \leq 10^6 R_{\odot}; \end{cases} \quad (1)$$

Especially important from the evolutionary point of view is how different are initial masses of the components (see e.g. Trimble (1983)). We have parametrized it by a power-law shape, assuming the primary mass to obey Salpeter’s power law:

$$f(M) = M_1^{-2.35}, \quad 0.1M_{\odot} < M_1 < 120M_{\odot}, \quad (2)$$

<sup>1</sup>E-mail: lipunov@xray.sai.msu.ru

<sup>2</sup>E-mail: pk@sai.msu.ru

<sup>3</sup>E-mail: mystery@xray.sai.msu.ru

<sup>4</sup>E-mail: a78b@yandex.ru

$$f(q) \sim q^{\alpha_q}, \quad q = M_2/M_1 < 1; \quad (3)$$

We should note that some apparently reasonable distributions – such as both the primary and secondary mass obeying Salpeter’s law, or “hierarchical” distributions involving the assumption that the total binary mass and primary’s mass are distributed according to the Salpeter mass function – all yield essentially flat-like distributions by the mass ratio (i.e. with our parameter  $\alpha_q \simeq 0$ ).

We assume that the neutron star is formed in the core collapse of the pre-supernova star. Masses of the young neutron stars are randomly distributed in the range  $M_{NS}^{min} - M_{NS}^{max}$ . Initial NS masses are taken to be in the range  $M_{NS} = 1.25 - 1.4M_\odot$ . The range of initial masses of the young NSs was based on the masses of the neutron star in the B1913+16 binary system and of the radio pulsar in the J0737-3039 binary. In the B1913+16 system (the Hulse-Taylor pulsar, radio pulsar + neutron star) the mass of the neutron star, which is definitely not accreting matter from the optical donor, is  $M_{NS} = 1.3873 \pm 0.0006M_\odot$  (Thorsett & Chakrabarty 1999; Wex et al. 2000; Weisberg & Taylor 2003). The mass of the pulsar in the J0737-3039 system (radio pulsar + radio pulsar), which likewise does not accrete from an optical companion, is  $M_{PSR} = 1.250 \pm 0.010M_\odot$  (Lyne et al. 2004). The mass range of stars producing neutron stars in the end of their evolution is assumed to be  $M_n - M_b$ ; stars with initial masses  $M > M_b$  are assumed to leave behind black holes;  $M_n$  is taken to be equal to  $10M_\odot$  in most cases (but in general this parameter is free). Note that according to some stellar models, a very massive star ( $\approx 50 - 100M_\odot$ ) can leave behind a neutron star as a remnant due to very strong mass loss via powerful stellar wind, so we account for this possibility in the corresponding models.

We take into account that the collapse of massive star into a neutron star can be asymmetrical, so that the newborn neutron star can acquire an additional, presumably randomly oriented in space kick velocity  $w$  (see Section 4 below for more details).

The magnetic field of rotating compact objects (neutron stars and white dwarfs) largely define the evolutionary stage of the compact object in a binary system (Shvartsman (1970);

Davidson & Ostriker (1973); Illarionov & Sunyaev (1975)), so we use the general classification of magnetic rotating compact objects (see e.g. Lipunov (1992)) in our calculations. The initial magnetic dipole moment of the newborn neutron star is taken according to the distribution

$$f(\log \mu) \propto \text{const}, \quad 10^{28} \leq \mu \leq 10^{32} \text{G cm}^3, \quad (4)$$

The initial rotational period of the newborn neutron star is assumed to be  $\sim 10$  ms.

It is not definitely clear as yet whether the magnetic field of neutron stars decays or not (see for a comprehensive review Chanmugam (1992)). We assume that the magnetic fields of neutron stars decays exponentially on a timescale of  $t_d$  (usually we take this parameter to be equal to  $10^8$ ,  $5 \cdot 10^7$  and  $10^7$  years). A radio pulsar is assumed to be “switched on” until its period  $P$  (in seconds) has reached the “death-line” defined by the relation  $\mu_{30}/P_d^2 = 0.4$ , where  $\mu_{30}$  is the dipole magnetic moment in units of  $10^{30} \text{G cm}^3$ .

We assumed that magnetic fields of neutron stars decay exponentially to minimal value  $B_{min} = 8 \cdot 10^7 \text{G}$  and do not decay further:

$$B = \begin{cases} B_0 \exp(-t/t_d), & t < t_d \ln(B_0/B_{min}), \\ B_{min}, & t \geq t_d \ln(B_0/B_{min}). \end{cases} \quad (5)$$

Parameters  $B_0$  and  $t_d$  in equation (5) are the initial field strength and the field decay time.

We also assume that the mass limit for neutron stars (the Oppenheimer-Volkoff limit) is  $M_{OV} = 2.0M_\odot$  (in general, it is a free parameter in the code; it depends on equation of state of the material of the neutron star).

The most massive stars are assumed to leave behind black holes after the collapse, provided that the progenitor mass before the collapse has a mass  $M_{cr}$ . The masses of the black holes are calculated as  $M_{bh} = k_{bh} M_{PreSN}$ , where the parameter  $k_{bh} = 0.0 - 1.0$ ,  $M_{PreSN}$  is the mass of the pre-supernova star.

We consider binaries with  $M_1 \geq 0.8M_\odot$  with a constant chemical (solar) composition. The process of mass transfer between the components is treated as conservative when appropriate, that is the total angular momentum of the binary system

is assumed to be constant. If the accretion rate from one component to another is sufficiently high (say, the mass transfer occurs on a timescale few times shorter than the thermal Kelvin-Helmholtz time for the normal companion) or a compact object is engulfed by a giant companion, the common envelope stage of binary evolution can begin (Paczynski 1976; van den Heuvel 1983).

Other cases of non-conservative evolution (for example, stages with strong stellar wind or those where the loss of binary angular momentum occurs due to gravitational radiation or magnetic stellar wind) are treated using the well known prescriptions (see e.g. Verbunt & Zwaan (1981); Rappaport et al. (1982); Lipunov & Postnov (1988)).

## 2. Evolutionary scenario for binary stars

Significant discoveries in the X-ray astronomy made during the last decades stimulated the astronomers to search for particular evolutionary ways of obtaining each type of observational appearance of white dwarfs, neutron stars and black holes, the vast majority of which harbours in binaries. Taken as a whole, these ways constitute a general evolutionary scheme, or the “evolutionary scenario”. We follow the basic ideas about stellar evolution to describe evolution of binaries both with normal and compact companions.

To avoid extensive numerical calculations in the statistical simulations, we treat the continuous evolution of each binary component as a sequence of a finite number of basic evolutionary states (for example, main sequence, red supergiant, Wolf-Rayet star, hot white dwarf, etc.), at which stellar parameters significantly differ from each other. The evolutionary state of the binary can thus be determined as a combination of the states of each component, and is changed once the more rapidly evolving component goes to the next evolutionary stage.

At each such stage, we assume that the star does not change its physical parameters (mass, radius, luminosity, the rate and velocity of stellar wind, etc.) that have effect on the evolution of the companion (especially in the case of compact magnetized stars). Every time the faster evolving component passes into the next stage, we recalculate its parameters. Depending on the evolution-

ary stage, the state of the slower evolving star is changed or can remain unchanged. With some exceptions (such as the common envelope stage and supernova explosion), states of both components cannot change simultaneously. Whenever possible we use analytical approximations for stellar parameters.

Prior to describing the basic evolutionary states of the normal component, we note that unlike single stars, the evolution of a binary component is not fully determined by the initial mass and chemical composition only. The primary star can fill its Roche lobe either when it is on the main sequence, or when it has a (degenerate) helium or carbon-oxygen core. This determines the rate of mass transfer to the secondary companion and the type of the remnant left behind. We will follow Webbink (1979) in treating the first mass exchange modes for normal binary components, whose scheme accounts for the physical state of the star in more detail than the simple types of mass exchange (A, B, C) introduced by Kippenhahn & Weigert (1967). We will use both notations A, B, C and D (for very wide systems with independently evolving companions) for evolutionary types of binary as a whole, and Webbink’s notations for mass exchange modes for each component separately [Ia], [Ib], [IIa], [IIb], [IIIa], etc.

## 3. Basic evolutionary states of normal stars

The evolution of a binary system consisting initially of two zero-age main sequence stars can be considered separately for each components until a more massive (primary) component fills its Roche lobe. Then the matter exchange between the stars begins.

The evolutionary states of normal stars will be denoted by Roman figures (I-IV), whereas those of compact stars will be marked by capital letters (E, P, A, SA ...). We divide the evolution of a normal star into four basic stages, which are significant for binary system evolution and bear a clear physical meaning. We will implicitly express the mass and radius of the star and the orbital semi-major axis in solar units ( $m \equiv M/M_\odot$ ,  $r \equiv R/R_\odot$ ,  $a \equiv A/R_\odot$ ), the time in million years, the luminosities in units of  $10^{38}$  erg  $s^{-1}$ , the wind velocities

in units of  $10^8 \text{ cm s}^{-1}$  and the accretion rates  $\dot{M}$  onto compact objects in units of  $10^{-8} M_\odot \text{ yr}^{-1}$ , unless other units are explicitly used.

### 3.1. Main sequence stars

At this stage, the star is on the zero-age main sequence (ZAMS) and its size is much smaller than the Roche lobe radius. The time the star spends on the main sequence is the core hydrogen burning time,  $t_H$ , which depends on the stellar mass only (Iben & Tutukov 1987):

$$\begin{cases} 1.0 + 0.95 \frac{79}{m}, & m \geq 79.0, \\ 10^{3.9 - 3.8 \log m + \log^2 m}, & 79 > m \geq 10, \\ 2400 m^{-2.16}, & 10 > m \geq 2.3, \\ 10^4 m^{-3.5}, & m < 2.3, \end{cases} \quad (6)$$

The radius of the ZAMS star is assumed to be

$$r = \begin{cases} 10^{0.66 \log m + 0.05}, & m > 1.12, \\ m, & m \leq 1.2, \end{cases} \quad (7)$$

and its luminosity is

$$\log L = \begin{cases} -5.032 + 2.65 \log m, & (\alpha) \\ -4.253 + 4.8 \log m, & (\beta) \\ -4.462 + 3.8 \log m, & (\gamma) \\ -3.362 + 3.0 \log m, & (\delta) \\ -3.636 + 2.7 \log m, & (\epsilon) \end{cases} \quad (8)$$

here we assume the next indication: ( $\alpha$ ),  $m < 0.6$ ; ( $\beta$ ),  $0.6 \leq m < 1.0$ ; ( $\gamma$ ),  $1.0 \leq m < 10.0$ ; ( $\delta$ ),  $10 \leq m < 48.0$ ; ( $\epsilon$ ),  $m \geq 48.0$ .

The initial mass of the primary and the mode of the first mass exchange (which is determined by the initial orbital period and masses of the components; see Webbink (1979)) determine the mass and the type of the core that will be formed during stage I. For example, for single stars and primaries in ‘‘type C’’ binaries that fill its Roche lobe having a degenerate core, we use the expressions

$$m_c = \begin{cases} 0.1 m_{max}, & (\alpha) \\ 0.446 + 0.106 m_{max}, & (\beta) \\ 0.24 m_{max}^{0.85}, & (\gamma) \\ \min(0.36 m_{max}^{0.55}, 0.44 m_{max}^{0.42}), & (\delta) \\ 0.44 m_{max}^{0.42}, & (\epsilon) \\ \approx M_{Ch}, & (\zeta) \\ 0.1 m_{max}^{1.4}, & (\eta) \end{cases} \quad (9)$$

where  $m_{max}$  is the maximum mass the star had during the preceding evolution. We assume the next indication in this formula: ( $\alpha$ ),  $m_{max} < 0.8$ ; ( $\beta$ ),  $0.8 \leq m_{max} < 2.3$ ; ( $\gamma$ ),  $2.3 \leq m_{max} < 4.0$ ; ( $\delta$ ),  $4.0 \leq m_{max} < 7.5$ ; ( $\epsilon$ ),  $7.5 \leq m_{max} < 8.8$ ; ( $\zeta$ ),  $8.8 \leq m_{max} < 10.0$ ; ( $\eta$ ),  $m_{max} \geq 10.0$ .

A main-sequence star accreting matter during the first mass transfer will be treated as a rapidly rotating ‘‘Be-star’’ with the stellar wind rate different from what is expected from a single star of the same mass (see below).

### 3.2. Post main-sequence stars

The star leaves the main sequence and goes toward the red (super)giant region. The star still does not fill its Roche lobe. The duration of this stage for a binary component is not any more a function of the stellar mass only (as in the case of single stars), but also depends on the initial binary type (A, B, or C) (see Iben & Tutukov (1985, 1987)):

$$t_{II} = \begin{cases} 0, & (\alpha), \\ 2t_{KH}, & (\beta), \\ 6300 m^{-3.2}, & (\gamma), \\ t_{He}, & (\delta), \end{cases} \quad (10)$$

In type A systems, the primaries fill their Roche lobes when they belong to the main sequence. We assume the next indication in this formula: ( $\alpha$ ), type A; ( $\beta$ ), type B excluding mode [IIIA]; ( $\gamma$ ), types C, D and mode [IIIA],  $m_{max} < 5$ ; ( $\delta$ ), types C, D and mode [IIIA],  $m_{max} > 5$ .

The radius of the post-MS star rapidly increases (on the thermal time scale) and reaches the characteristic giant values. The star spends the most time of helium burning with such large radius. In the framework of our approximate description, we take the radius of the giant star to be equal to the maximum value, which depends strongly on the mass of its core and is calculated according to Webbink’s mass transfer modes as follows (see also Iben & Tutukov (1985, 1987)):

$$r_{II} = \begin{cases} 3000 m_c^4, & (\alpha) \\ 1050 (m_c - 0.5)^{0.68}, & (\beta) \\ 10 m_c^{0.44}, & (\gamma) \end{cases} \quad (11)$$

We assume the next indication in this formula: ( $\alpha$ ), mode [IIIA] or [IIIB] with He core; ( $\beta$ ),

mode [IIIB] with CO or ONeMg core; ( $\gamma$ ), modes [I] or [II]. Formula (11) depicts stars with mass  $\leq 10M_\odot$ .

This maximum radius can formally exceed the Roche lobe size; in such cases we put it equal to  $0.9R_L$  during the stage II. The most sensitive to this crude approximation are binaries with compact companions, which can lead, for example, to the overestimation of the number of accreting neutron stars observed as X-ray pulsars. However, these stages are less important for our analysis than the stages at which the optical star fills its Roche lobe. A more detailed treatment of normal star evolution (given, for example, by Pols & Marinus (1994)) can reduce such uncertainties.

Luminosities of giants are taken from de Jager (1980):

$$\log l_{II} = \begin{cases} \frac{15.92m_c^6}{(1.0+m_c^4)(2.512+3.162m_c)}, & (\alpha) \\ 10^{-4.462+3.8 \log m}, & (\beta) \\ 10^{-3.362+3.0 \log m}, & (\gamma) \\ 10^{-3.636+2.7 \log m}, & (\delta) \end{cases} \quad (12)$$

We assume the next indication in this formula: ( $\alpha$ ),  $m < 23.7$ ,  $m_c < 0.7$ ; ( $\beta$ ),  $m < 23.7$ ,  $m_c > 0.7$ ; ( $\gamma$ ),  $48 > m > 23.7$ ; ( $\delta$ ),  $m > 48$ .

Radii of (super)giants are determined by using the effective temperature  $T_{eff}$  and luminosities. Typical effective temperatures are taken from Allen (1973):

$$\log T_{eff} = \begin{cases} 4.50, & (\alpha) \\ 3.60, & (\beta) \\ 3.70, & (\gamma) \end{cases} \quad (13)$$

We assume the next indication in this formula: ( $\alpha$ ),  $m > 10.0$ ; ( $\beta$ ),  $m < 10.0$ , type C or D; ( $\gamma$ ),  $m < 10.0$ , type A or B. So, we calculate  $R_{II}$  with mass higher than  $10M_\odot$  calculate using formula

$$r_{II} = \exp \{2.3(0.5 \log l_{ii} - 2 \log T_{eff} + 9.7)\}. \quad (14)$$

### 3.3. Roche lobe overflow

At this stage the star fills its Roche lobe (RL) and mass transfer onto the companion occurs. The mass transfer first proceeds on the thermal

time scale (see extensive discussion of this approximation in van den Heuvel (1994))

$$t_{KH} \sim 30m^2r_*^{-1}(L/L_\odot)^{-1}, \quad (15)$$

The common envelope stage (CE) may be formed if the Roche lobe overflow occurs in the type C system (where the primary has a well developed core) even for  $q < 1$ ; otherwise (for type B systems) we use the condition  $q \leq q_{cr} = 0.3$  for the CE stage to occur. Radius of the star at the Roche lobe filling stage is taken to be that of the equivalent Roche lobe radius (Eggleton 1983):

$$\frac{R_L}{a(1-e)} = \frac{0.49q^{2/3}}{0.6q^{2/3} + \ln(1+q^{1/3})}, \quad (16)$$

Here  $a$  is the binary orbital separation and  $e$  is the orbital eccentricity,  $q$  is the arbitrary mass ratio.

For  $q < 0.6$  a more precise approximation can be used:

$$\frac{R_L}{a} = 0.4622 \left( \frac{q}{1+q} \right)^{1/3}. \quad (17)$$

A star filling its Roche lobe has quite different boundary conditions in comparison with single stars. The stellar radius at this stage is limited by the Roche lobe. If the stellar size exceeds the Roche lobe, the star can lose matter on a time scale close to the dynamical one until its radius becomes smaller than the new Roche lobe size.

Now we consider how the RL-filling star loses matter. Let the star be in equilibrium and  $R_{eq}(M) = R_L(M)$  at the initial moment of time. When a fraction of mass  $\delta m$  is transported to the companion, the mass ratio  $q$  and semi-major axis  $a$  of the binary changes depending on the mass transfer mode assumed (see below for details). The RL size then becomes equal to  $R_L(M - \delta m)$ .

On the other hand, mass loss disturbs equilibrium of the star (hydrodynamical and thermal). The hydrodynamical equilibrium is restored on the dynamical timescale  $t_d \propto (GM/R^3)^{-1/2}$ . The stellar radius changes to a value  $R_{ad}(M - \delta m)$  (where ‘‘ad’’ means adiabatic), which can be bigger or smaller than the equilibrium radius  $R_{eq}(M - \delta m)$  of the star. The thermal equilibrium establishes on the thermal time scale  $T_{KH} \approx$

$GM^2/R_L$ , so after that the stellar radius relaxes to the equilibrium value  $R_{eq}(M - \delta m)$ .

Relations  $R_L(M - \delta m)$ ,  $R_{ad}(M - \delta m)$  and  $R_{eq}(M - \delta m)$  determine the mode of mass transfer during the RL overflow stage. Following Webbink (1985), one usually introduces the logarithmic derivative  $\zeta = d \ln R / d \ln M$  ( $R \propto M^\zeta$ ). It locally fits the real dependence  $R(M)$ . Three values of  $\zeta$  are relevant:

$$\begin{aligned}\zeta_L &= \frac{d \ln R_L}{d \ln M}, \\ \zeta_{ad} &= \frac{d \ln R_{ad}}{d \ln M}, \\ \zeta_{eq} &= \frac{d \ln R_{eq}}{d \ln M},\end{aligned}\tag{18}$$

where “ $L$ ”, “ $ad$ ” and “ $eq$ ” correspond to the values of radii discussed above.

Three possible cases are considered depending on  $\zeta_i$ :

1. If  $\zeta_{ad} < \zeta_L$ , the star cannot be inside its RL regardless of the mass loss rate ( $dM/dt < 0$ ). Such stars lose their matter in hydrodynamical time scale. Mass loss rate is limited only by the speed of sound near the inner Lagrangian point  $L_1$ .  $\zeta_{eq}$  is unimportant because the size of the star becomes bigger and bigger than  $R_L$ . The equilibrium is impossible.
2.  $\zeta_{eq} < \zeta_L < \zeta_{ad}$ . The star losing mass cannot be in thermal equilibrium, because otherwise its size would exceed  $R_L$ . Nevertheless, in this case  $R_{ad} < R_L$ . So the hydrodynamical equilibrium is established. As a result, the star loses mass on thermal time scale.
3.  $\zeta_L < \zeta_{ad}, \zeta_{eq}$ . In this case the size of the star losing mass becomes smaller than its RL. The evolutionary expansion of the star or the binary semi-major axis decrease due to orbital angular momentum loss via magnetic stellar wind (MSW) or gravitational radiation (GW) support the permanent contact of the star with RL. The star then loses mass on a time scale dictated by its own evolutionary expansion or on a time scale corresponding to the orbital angular momentum loss.

For non-degenerate stars,  $R_{eq}$  increases monotonically with  $M$ . On the other hand, the exponent  $\zeta_{ad}$  is determined by the entropy distribution over the stellar radius which is different for stars with radiative and convective envelopes. It can be shown that stars with radiative envelopes should shrink in response to mass loss, while those with convective envelopes should expand<sup>5</sup>.

Therefore, stars with convective envelopes in binaries should generally have a higher mass loss rate than those with radiative envelopes under other equal conditions. The next important factor is the dependence  $R_L(M)$ . It can be found by substituting one of the relations  $a(M)$  (see below) into equation (16) or into equation (17) and differentiating it with respect to  $M$ . For example, assuming the conservative mass exchange when the total mass and the orbital angular momentum of the system do not change, one readily gets that the binary semi-major axis decreases when the mass transfer occurs from the more massive to the less massive component;  $R_L$  decreases of the primary correspondingly. When the binary mass ratio reaches unity, the semi-major axis takes on a minimal value. In contrast, if the less massive star loses its mass conservatively the system expands. In that case the mass transfer can be stable.

If more massive component with radiative envelope fills its RL, the mass transfer proceeds on thermal time scale until the masses of the components become equal<sup>6</sup>. The next stage of the first mass exchange proceeds in more slower (nuclear) time scale. If the primary has convective envelope, the mass transfer can proceed much faster on a time scale intermediate between the thermal and hydrodynamical one, and probably on the hydrodynamical time scale. In that case the fast stage of the mass exchange ends when the mass of the donor decreases to  $\sim 0.6$  mass of the secondary companion (Tutukov & Yungelson 1973). Further mass transfer should proceed on the evolutionary time scale.

<sup>5</sup>The adiabatic convection in stellar envelope can be described by the polytropic equation of state  $P \propto \rho^{5/3}$ , similar to non-relativistically degenerate white dwarfs. For such equation of state the mass-radius relation becomes inverse:  $R \propto M^{-1/3}$ . For non-degenerate stars with convective envelopes this relation holds approximately.

<sup>6</sup>The mass exchange can stop earlier if the entire envelope is lost and the stellar core is stripped (the core has other values  $\zeta_{ad}$  and  $\zeta_{eq}$ ).

The process of mass exchange strongly depends on stellar structure at the moment of the RL overflow. The structure of the star in turn depends on its age and the initial mass. The moment of the RL overflow is determined by the mass of the components and by the initial semi-major axis of the system. to calculate a diagram in the  $M - a$  (or  $M - P_{orb}$ ) plane which allows us to conclude when the primary in a binary with given initial parameters fills its RL, what is its structure at that moment and what type of the first mass exchange is expected. We use the diagram calculated by Webbink (1979) (see also the description of modern stellar wind scenarios below).

We distinguish different sub-stages of the RL overflow according to the characteristic timescales of the mass transfer:

**stage III:**

This is the most frequent case for the first mass transfer phase. The primary fills its RL and the mass transfer proceeds faster than evolutionary time scale (if outer layers of the star are radiative, then it is thermal time scale, if outer layers are convective, then time scale is shorter, up to hydrodynamical time scale). This stage comes to the end when mass ratio in the system changes (“role-to-role transition”), i.e. when the mass of the donor (mass losing) star is equal to mass of second companion (for radiative envelopes) or 0.6 of the mass of the second companion (for convective envelopes). This stage also stops if the donor star totally lost its envelope.

**stage IIIe:**

This is the slow (evolutionary driven) phase of mass transfer. We assume it to occur in short-period binaries of type A. However, it is not excluded that it may occur after the mass reversal during the first stage of mass exchange for binaries of type B (see van den Heuvel (1994)), e.g. as in wide low-mass X-ray binaries.

**stage IIIs**

This is the specific to super-accreting compact companions substage of fast mass transfer at which matter escapes from the secondary companion carrying away its orbital angular momentum. Its duration is equal to

$$t_{III_s} = t_{KH} \frac{q(1+q)}{2-q-2q^2}, \quad (19)$$

$$q = M_a/M_d < 0.5,$$

here and below subscripts “a” and “d” refer to the accreting and donating mass star, respectively. For systems with small mass ratios,  $q < 0.5$ , this timescale corresponds to an effective  $q$ -time shortening of the thermal time for the RL-overflowing star.

**stages III<sub>m,g</sub>**

At these stages, the mass transfer is controlled by additional losses of orbital angular momentum  $J_{orb}$  caused by magnetic stellar wind or gravitational wave emission. The characteristic time of the evolution is defined as  $\tau_J = -(J_{orb}/\dot{J}_{orb})$ , and in the case of MSW is (see Verbunt & Zwaan (1981); Iben & Tutukov (1987))

$$\tau_{MSW} = 4.42 \frac{a^5 m_x \lambda_{MSW}^2}{(m_1 + m_2)^2 m_{op}^4}, \quad (20)$$

Here  $m_{op}$  denotes mass of the low-mass optical star ( $0.3 < m < 1.5$ ) that is capable of producing an effective magnetic stellar wind (because only such stars have outer convective envelopes which are prerequisite for effective MSW),  $\lambda$  is a numerical parameter of order of unity. We have used the mass-radius relation  $r \approx m$  for main sequence stars in deriving this formula. The upper limit of the mass interval and empirical braking law for main-sequence G-stars are taken from Skumanich (1972), the lower limit is determined by absence of cataclysmic variables with orbital periods  $P_{orb} \approx 3^h$  (Verbunt 1984; Mestel 1952; Kawaler 1988; Tout & Pringle 1992; Zangrilli et al. 1997). We use  $\lambda = 1$  (see for details Kalogera & Webbink (1998)).

The time scale of the gravitational wave emission is

$$\tau_{GW} = 124.2 \frac{a^4}{m_1 m_2 (m_1 + m_2)} \times \left( 1 + \frac{73}{24} e^2 + \frac{37}{96} e^4 \right) (1 - e^2)^{-7/2}, \quad (21)$$

Whether the evolution is governed by MSW or GW is decided by which time scale ( $\tau_{MSW}$  or  $\tau_{GW}$ ) turns out to be the shortest among all appropriate evolutionary time scales.

**stage III<sub>wd</sub>**

This is a special case where the white dwarf overflows its RL. This stage is encountered for very

short period binaries (like Am CVn stars and low-mass X-ray binaries like 4U 1820-30) whose evolution is controlled by GW or MSW. The mass transfer is calculated using the appropriate time scale (GW or MSW). The radius of the white dwarf increases with mass  $R_{WD} \propto M^{-1/3}$ . This fact, however, does not automatically imply that the mass transfer is unstable, since the less massive WD fills its RL first. It can be shown that the mass exchange is always stable in such systems if the mass ratio  $q < 0.8$ . This condition always holds in WD+NS and WD+BH systems. WD loses its matter until its mass decreases to that of a huge Jupiter-like planet ( $\sim$  a few  $10^{-3}M_{\odot}$ ), where the COulomb interaction reverses the mass-radius relation  $R(M)$ . Such a planet can approach the secondary companion of the system due to GW emission until the tidal forces destroy it completely. The matter of the planet can fall onto the surface of the second companion in form a long-living disk around it. If the second star is a neutron star and its rotation had been spun up by accretion such that a millisecond radio pulsar appeared, the planet can be evaporated by relativistic particles emitted by the pulsar (Paczynski & Sienkiewicz 1983; Joss & Rappaport 1983; Kolb et al. 1998; Kalogera & Webbink 1998).

The mass loss rate at each of the III-stages is calculated according to the relation

$$\dot{M} = \Delta M / \tau_i, \quad (22)$$

where  $\Delta M$  is the *a priori* known mass to be lost during the mass exchange phase (e.g.  $\Delta M = M_1 - (M_1 + M_2)/2$  in the case of the conservative stage III, or  $\Delta M = M_1 - M_{core}(M_1)$  in case of III(e,m,g) or CE) and  $\tau_i$  is the appropriate time scale.

The radius of the star at stage III is assumed to follow the RL radius:

$$R_i^d(M_d(t)) = R_d(M_d(t)). \quad (23)$$

### 3.4. Wolf-Rayet and helium stars

In the process of mass exchange the hydrogen envelope of the star can be lost almost completely, so a hot white dwarf (for  $m \leq 2.5$ ), or a non-degenerate helium star (for higher masses) is left as a remnant. The life-time of the helium star is determined by the helium burning in the stellar core (Iben & Tutukov 1985)

$$t_{He} = \begin{cases} 1658m^{-2}, & (\alpha) \\ 1233m^{-3.8}, & (\beta) \\ 0.1t_H, & (\gamma) \\ 6913m^{-3.47}, & (\delta) \\ \simeq 10, & (\epsilon) \\ 0.1t_H, & (\zeta) \end{cases} \quad (24)$$

We assume the next indication in this formula: ( $\alpha$ ),  $m < 1.1$ , modes [IIA-IIIF]; ( $\beta$ ),  $m > 1.1$ ,  $m_{max} < 10$ , modes [IIA-IIIF]; ( $\gamma$ ),  $m_{max} > 10$ , modes [IIA-IIIF]; ( $\delta$ ), mode [IIIA]; ( $\epsilon$ ), mode [IIIC]; ( $\zeta$ ), modes [IIIB,D,E] and type D.

If the helium (WR) star fills its Roche lobe (a relatively rare so-called ‘‘BB’’ case of evolution; Delgado & Thomas (1981); see discussion in van den Heuvel (1994)), the envelope is lost and a CO stellar core is left with mass

$$m_c = \begin{cases} 1.3 + 0.65(m - 2.4), & m \geq 2.5, \\ 0.83m^{0.36}, & m < 2.5, \end{cases} \quad (25)$$

The mass-radius dependence in this case is (Tutukov & Yungelson 1973)

$$r_{WR} = 0.2m^{0.6}. \quad (26)$$

### 3.5. Stellar winds from normal stars

The effect of the normal star on the compact magnetized component is largely determined by the rate  $\dot{M}$  and the velocity of stellar wind at infinity  $v_{\infty}$ , which is assumed to be

$$v_{\infty} = 3v_p \approx 1.85\sqrt{m/r}, \quad (27)$$

where  $v_p$  is the escape velocity at the stellar surface.

For ‘‘Be-stars’’ (i.e. those stars at the stage ‘‘I’’ that increased its mass during the first mass exchange), the wind velocity at the infinity is taken to be equal to the Keplerian velocity at the stellar surface:

$$v_{\infty} = \sqrt{GM/R} \approx 0.44\sqrt{m/r}. \quad (28)$$

The lower stellar wind velocity leads to an effective increase of the captured mass rate by the secondary companion to such ‘‘Be-stars’’.

The stellar wind mass loss rate at the stage ‘‘I’’ is calculated as

(de Jager 1980)

$$\dot{m} = 52.3\alpha_w l / v_\infty, \quad (29)$$

Here  $\alpha_w = 0.1$  is a numerical coefficient (in general, we can treat it as free parameter).

For giant post-MS stars (stage “II”) we assume  $v_\infty = 3v_p$  and for massive star we take the maximum between the stellar wind rate given by de Jager’s formula and that given by Lamers (1981)

$$\dot{m} = \max\left(52.3\alpha_w \frac{l}{v_\infty}, 10^{2.33} \frac{l^{1.42} r^{0.61}}{m^{0.99}}\right), \quad (30)$$

$$M \geq 10M_\odot;$$

For red super-giants we use Reimers’s formula (Kudritzki & Reimers 1978):

$$\dot{m} = \max\left(52.3\alpha_w \frac{l}{v_\infty}, 1.0 \frac{lr}{m}\right), \quad (31)$$

$$M \geq 10M_\odot;$$

For a Wolf-Rayet star the stellar wind loss rate can significantly increase (up to  $10^{-5}M_\odot \text{ year}^{-1}$ ). We parametrize it as

$$\dot{M}_{WR} = k_{WR} M_{WR} / t_{He}, \quad (32)$$

where the numerical coefficient is taken to be  $k_{WR} = 0.3$  (in general, it can be changed if necessary). The mass loss in other stages (MS, (super)giant) is assumed to be limited by 10% of the mass of the star at the beginning of the stage.

### 3.6. Change of binary parameters: mass, semi-major axis and eccentricity

The duration of any evolutionary stage is determined by the more rapidly evolving component  $\Delta t = \min(\Delta t_1, \Delta t_2)$ . On the other hand, based on the evolutionary considerations we are able to calculate how the mass of the faster evolving star changes (e.g. due to the stellar wind or RL overflow), that is we can estimate the quantity  $\Delta M = M_i - M_f$ . Then we set the characteristic mass loss rate at this stage as

$$\dot{M}_o = \Delta M / \Delta t, \quad (33)$$

Next, we should calculate the change of mass for the slower evolving companion, the orbital semi-major axis and the eccentricity.

### 3.7. Mass change

The mass of the star losing matter is calculated as

$$M_f = M_i - \dot{M}_o \times \Delta t, \quad (34)$$

Accordingly, the mass of the accreting star is

$$M_f = M_i + \dot{M}_c \times \Delta t, \quad (35)$$

where  $\dot{M}_c$  is the accretion rate of the captured matter.

For stages without RL overflow the accretion rate of the captured stellar wind matter is

$$\dot{m}_c = 3.8 \times 10^{-2} \left( \frac{m}{a(v_w^2 + 0.19(m_1 + m_2)/a)} \right)^2 \dot{m}_o. \quad (36)$$

At stages where RL overflow occurs and both components are normal (non-degenerate), we will assume that the accretor can accommodate mass at the rate determined by its thermal time, i.e.

$$\dot{m}_c = \dot{m}_o \left( \frac{t_{KH}(\text{donor})}{t_{KH}(\text{accretor})} \right). \quad (37)$$

This means that the evolution can not be fully conservative, especially during the first mass transfer where the primary component usually has a shorter thermal time scale.

The mass increase rate by compact accretors is assumed to be limited by the critical Eddington luminosity (see, however, the possible hyper accretion stage discussed below):

$$L_{Edd} = \frac{4\pi GMm_p}{\sigma_T} \approx 1.3 \cdot 10^{38} \times m \text{ erg/s} \quad (38)$$

( $\sigma_T$  is the Thomson cross-section) at the stopping radius  $R_{stop}$  for the accreted matter (see, e.g., detailed discussion in Lipunov (1992)). This corresponds to the critical accretion rate

$$\dot{M}_{cr} = R_{stop} \frac{L_{Edd}}{GM}. \quad (39)$$

Thus, the mass of the accreting compact star at the end of the stage is determined by the relation

$$M_f = M_i + \min(\dot{M}_c, \dot{M}_{cr}) \times \Delta t. \quad (40)$$

### 3.8. Semi-major axis change

The binary separation  $a$  changes differently for various mass exchange modes. First, we introduce a measure of non-conservativeness of the mass exchange as the ratio between the mass change of the accretor and the donor:

$$\beta \equiv -(M_{accretor}^i - M_{accretor}^f)/(M_{donor}^i - M_{donor}^f). \quad (41)$$

If the mass exchange is conservative ( $\beta = 1$ , i.e.  $M_a + M_d = \text{const}$ ) and one can neglect the angular momenta of the components, the orbital momentum conservation implies

$$\frac{a_f}{a_i} = \left( \frac{M_a^i M_d^i}{M_a^f M_d^f} \right)^2. \quad (42)$$

In a more general case of quasi-conservative mass transfer  $0 \leq \beta < 1$ , the orbital separation changes differently depending on the specific angular momentum carried away from the system by the escaping matter (see van den Heuvel (1994) for more detail). We treat the quasi-conservative mass transfer by assuming the isotropic mass loss mode in which the matter carries away the specific orbital angular momentum of the accreting component ( $j_a$ )

$$\dot{J}_{out} = (1 - \beta)\dot{M}_c j_a. \quad (43)$$

From here we straightforwardly find

$$\frac{a_f}{a_i} = \left( \frac{q_f}{q_i} \right)^3 \left( \frac{1 + q_i}{1 + q_f} \right) \left( \frac{1 + \frac{\beta}{q_f}}{1 + \frac{\beta}{q_i}} \right)^{3+2/\beta}. \quad (44)$$

In this formula  $q = M_{accretor}/M_{donor}$  and the non-conservative parameter  $\beta$  is set to be the minimal value between  $\beta = 1$  and the ratio  $T_{KH}(donor)/T_{KH}(accretor)$  ( $T_{KH}(donor)$  and  $T_{KH}(accretor)$  is the thermal time of donor and accretor, respectively).

When no matter is captured by the secondary companion without additional losses of angular momentum (the so-called ‘‘absolutely non-conservative case’’), which relates to the spherical-symmetric stellar wind from one component, we use another well-known formula

$$\frac{a_f}{a_i} = \frac{M_1^i + M_2^i}{M_1^f + M_2^f}. \quad (45)$$

In this case the orbital separation always increases.

When the orbital angular momentum is carried away by GW or MSW with no RL overflow, the following approximate formulas are used:

$$\frac{a_f}{a_i} = \begin{cases} (1 - \Delta t/\tau_{MSW})^{1/4}, & \text{for MSW,} \\ (1 - \Delta t/\tau_{GW})^{1/5}, & \text{for GW,} \end{cases} \quad (46)$$

In a special case of a white dwarf filling its RL (stage ‘‘IIIwd’’ above), assuming a stable (i.e. where  $d \ln R_{wd}/d \ln M = d \ln R_{RL}/d \ln M$ ) conservative mass transfer with account for the mass-radius relation  $R_{wd} \propto M_{wd}^{-1/3}$ , the orbital separation must increase according to the equation

$$\frac{a_f}{a_i} = \left( \frac{m_f}{m_i} \right)^{-2/3}, \quad (47)$$

where  $m_i$  is the initial mass of the WD donor and  $m_f$  is its mass at the end of the mass transfer.

### 3.9. The change of eccentricity

Tidal interaction between components, as well as the orbital angular momentum loss due to MSW or GR decrease the eccentricity of the binary system. The tidal interaction is essential in very close binaries or even during the common envelope stage. MSW is effective only in systems with low-mass late-type main sequence stars (see above), GW losses become significant only in short-period binaries.

The tidal interaction conserves the orbital angular momentum which implies the relation

$$a(1 - e^2) = \text{const.} \quad (48)$$

It seems that the orbit becomes a circle faster than major semi-axis of the orbit decreases during common envelope stage. We suppose that  $t_{cyr} = 1/3t_{CE}$ . We accept that  $t_{cyr}$  for RL-filling stars is equal to its Kelvin-Helmholtz time. Detached systems change their eccentricity during the next character time (Zahn 1975; Press & Teukolsky 1977; Zahn 1989b; Zahn & Bouchet 1989b)

$$t_{cyr} = t_{KH} \left( \frac{1 + e}{1 - e} \right)^{3/2} \left( \frac{R}{R_L} \right)^{-5}. \quad (49)$$

here  $t_{KH} \approx GM^2/R_L$  is thermal time of the star,  $R$  is radius of the star,  $R_L$  is its RL size. For systems which consist of two normal stars we choose minimal value of  $t_{cyr}$ . Resonances at very high eccentricities are not taken into account (Mardling 1995a,b).

Orbits of the systems with MSW become circular during  $t_{cyr} = \tau_{MSW}$  (see 46).

In case of GW analytical exact solutions were obtained for  $a(t)$  and  $e(t)$  (Peters & Mathews 1963; Peters 1964).

#### 4. Special cases: supernova explosion and common envelope

Supernova explosion in a binary is treated as an instantaneous mass loss of the exploding star. The additional kick velocity can be imparted to the newborn neutron star due the collapse asymmetry (see below for discussion). In this case the eccentricity and semi-major axis of the binary after the explosion can be straightforwardly calculated (Boersma 1961) (see necessary formulas also in Grishchuk et al. 2001). Briefly, we use the following scheme.

1. First, velocities and locations of the components on the orbit prior to the explosion are calculated;
2. then the mass of the exploding star  $M_{pr}$  -  $M_{remnant}$  is changed and the arbitrarily directed kick velocity  $w$  is added to its orbital velocity;
3. after that the transition to the new system's barycenter is performed (at this point the spatial velocity of the new center of mass of the binary is calculated);
4. in this new reference frame the new total energy  $E'_{tot}$  and the orbital angular momentum  $J'_{orb}$  are computed; if the new total energy is negative, the new semi-major axis  $a'$  and eccentricity  $e'$  are calculated by using the new  $J'_{orb}$  and  $E'_{tot}$ ; if the total energy is positive (that is, the binary is unbound) spatial velocities of each component are calculated.

The kick velocity  $w$  distribution is taken in the Maxwellian form:

$$f(w) \sim \frac{w^2}{w_0^2} e^{-\frac{w^2}{w_0^2}}. \quad (50)$$

We suppose that the absolute value of the velocity that can be added during the formation of a black hole depends on the mass loss by the collapsing star, the value of the parameter  $w_0$  during the BH formation is defined as

$$w_0^{bh} = (1 - k_{bh}) w_0. \quad (51)$$

An effective spiral-in of the binary components occurs during the common envelope (CE) stage. This complicated process (introduced by Paczynski (1976)) is not fully understood as yet, so we use the conventional energy consideration to find the binary system parameters after the CE by introducing a parameter  $\alpha_{CE} = \Delta E_b / \Delta E_{orb}$ , where  $\Delta E_b = E_{grav} - E_{thermal}$  is the binding energy of the ejected envelope matter and  $\Delta E_{orb}$  is the drop in the orbital energy of the system during the spiral-in phase (van den Heuvel 1994). This parameter measures the fraction of the system's orbital energy that comes during the spiral-in process to the binding energy (gravitational minus thermal) of the ejected common envelope. Thus

$$\alpha_{CE} \left( \frac{GM_a M_c}{2a_f} - \frac{GM_a M_d}{2a_i} \right) = \frac{GM_d (M_d - M_c)}{R_d}, \quad (52)$$

where  $M_c$  is the mass of the core of the mass-losing star with the initial mass  $M_d$  and radius  $R_d$  (which is simply a function of the initial separation  $a_i$  and the initial mass ratio  $M_a/M_d$ , where  $M_a$  is the mass of the accreting star).

On the CE stage the luminosity of the accreting star can reach the Eddington limit so that the further increase of the accretion rate can be prevented by radiation pressure. This usually happens at accretion rates  $\dot{M} \simeq 10^{-4} - 10^{-5} M_\odot \text{ yr}^{-1}$ . However, Chevalier (1993) suggested that when the accretion rate is higher ( $\dot{M} \simeq 10^{-2} - 10^{-3} M_\odot \text{ yr}^{-1}$ ), the energy is radiated away not by high-energy photons only, but also by neutrinos (see also Zeldovich et al. (1972) and the next section). On the typical time scale for the hyper accretion stage of  $10^2 \text{ yr}$ , up to  $\sim 1 M_\odot$  of matter may be incident onto the surface of the neutron star.

## 5. Three regimes of mass accretion by neutron stars

A considerable fraction of observed neutron stars have increased their masses in the course of their evolution, or are still increasing their masses (e.g., in X-ray sources). But how large can this mass increase be? It is clear that the only origin of a mass increase is accretion. It is evident that the overall change in the mass of a neutron star is determined not only by the accretion rate, but also by the duration of the accretion stage:

$$\Delta M = \int_0^{T_a} \dot{M} dt = \dot{M} T_a, \quad (53)$$

where  $\dot{M}$  is the mean accretion rate and  $T_a$  is the lifetime of the accretion stage. We emphasize that, in the case under consideration, the accretion rate is the amount of matter falling onto the surface of the neutron star per unit time, and can differ significantly from the values indicated by the classical Bondi-Hoyle formulas. Three regimes of accretion are possible in a close binary containing a neutron star: ordinary accretion, super-accretion, and hyper-accretion.

### 5.1. Ordinary accretion

The ordinary accretion regime is realized when all matter captured by the gravitational field of the neutron star falls onto its surface. This is possible only if the radiation pressure and electromagnetic forces associated with the magnetic field of the star and its rotation are small compared to the gravitational force. In this case, the increase in the mass will be precisely determined by the gas dynamics of the accretion at the gravitational-capture radius or, if the donor fills its Roche lobe, by the binary mass ratio and the evolutionary status of the optical component. In this case, the accretor is observed as an X-ray source with luminosity

$$L_x = \dot{M} \frac{GM_x}{R_*}, \quad (54)$$

where  $M_x$  and  $R_*$  are the mass and radius of the neutron star. The accretion rate  $\dot{M}$  is determined by the Bondi-Hoyle formula

$$\dot{M} = \pi R_G^2 \rho v, \quad (55)$$

where  $R_G$  is the gravitational-capture radius of the neutron star,  $v$  is the velocity of the gas flow relative to the neutron star, and  $\rho$  is the density of the gas.

The X-ray luminosity of the accretor  $L_x$  and its other main parameters can be used to estimate the mass  $\Delta M$  accumulated during the accretion phase:

$$\Delta M = \frac{L_x R_* T_a}{GM_x}, \quad (56)$$

### 5.2. Super-accretion

Regime of super accretion was considered, for instance, in paper Lipunov (1982d). Despite the absence of detailed models for supercritical disk accretion (supercritical accretion is realized precisely via an accretion disk), it is possible to estimate the main characteristics of the process – the accretion rate, magnetosphere radius, and evolution equations. Accretion is considered to be supercritical when the energy released at the radius where the accretion exceeds the Eddington limit:

$$\dot{M} \frac{GM_x}{R_{stop}} > L_{Edd} = 1.38 \times 10^{38} (M_x/M_\odot) \text{ erg s}^{-1}, \quad (57)$$

where  $R_{stop}$  is either the radius of the neutron star or the magnetosphere radius  $R_A$ .

For strongly magnetized neutron stars with magnetic fields  $B \gg 10^8$  G, all matter arriving at the magnetosphere is accreted onto the magnetic poles, where the corresponding gravitational energy is released. If the black body temperature  $T$ , roughly estimated as

$$S\sigma T^4 = \dot{M} \frac{GM_x}{R_*}, \quad (58)$$

is higher than  $5 \times 10^9$  K ( $S$  is the area of the base of the accretion column), most of the energy will escape from the neutron star in the form of neutrinos, and, hence, will not hinder accretion (Zeldovich et al. 1972; Basko & Sunyaev 1975). In this case, the rate at which the neutron star accumulates mass will be

$$\dot{M} \simeq \dot{M}_{crit} \left( \frac{R_A}{R_*} \right)^2 \gg \dot{M}_{crit}, \quad (59)$$

For lower temperatures there should be an upper limit on the accretion rate equal to the standard Eddington limit.

### 5.3. Hyper-accretion

A considerable fraction of neutron stars in binary systems pass through the common-envelope stage in the course of their evolution. In this case, the neutron star is effectively immersed in its optical companion, and for a short time ( $10^2$ - $10^4$  yrs) spirals-in inside a dense envelope of the companion. The formal accretion rate estimated using the Bondi-Hoyle formulas is four to six orders of magnitude higher than the critical rate and, as was suggested by Chevalier (1993), this may result in hyper-accretion, when all the energy is carried away by neutrinos for the reasons described above. There are currently no detailed theories for hyper-accretion or the common-envelope stage. The amount of matter accreted by the neutron star can be estimated as

$$\begin{aligned} \Delta M &= \int_0^{T_{hyper}} \frac{1}{4} \left( \frac{R_G}{a} \right)^2 \dot{M} dt \simeq \quad (60) \\ &\simeq \frac{1}{4} (M_{opt} - M_{core}) \left( \frac{M_x}{M_{opt}} \right)^2 ; \end{aligned}$$

where  $T_{hyper}$  is the duration of the hyper-accretion stage,  $R_G$  is the gravitational-capture radius of the neutron star,  $a$  is the initial semi-major axis of the close binary orbit,  $M_{core}$  is the mass of the core of the optical star, and  $M_{opt}$  and  $M_x$  are the total masses of the optical star and of the neutron star at the onset of the hyper-accretion stage. The mass of the neutron star can increase during the common envelope stage as much as  $\sim 1M_\odot$  (Bogomazov et al. 2005), up to  $M_{OV}$ . Such NSs collapse into black holes.

### 6. Mass accretion by black holes

If the black hole has formed in the binary system, its X-ray luminosity is

$$L_x = \mu \dot{M} c^2, \quad (61)$$

where  $\mu = 0.06$  for Schwarzschild black hole and  $\mu = 0.42$  (maximum) for extremal Kerr BH.

We use the Bondi-Hoyle formulas to estimate the accretion rate onto BH.

Powerful X-ray radiation is able to originate only if an accretion disc has formed around the black hole (Karpov & Lipunov 2001). For spherically symmetric accretion onto a black hole the X-ray luminosity is insignificant. A very low stellar wind velocity is necessary to form an accretion disc (Lipunov 1992)

$$\begin{aligned} V &< V_{cr} \approx \quad (62) \\ &\approx 320(4\eta)^{1/4} m^{3/8} T_{10}^{-1/4} R_8^{-1/8} (1 + \tan^2 \beta)^{-1/2}, \end{aligned}$$

where  $\eta$  is averaged over the z-coordinate dynamic viscous coefficient,  $m = M_x/M_\odot$ ,  $M_x$  is the relativistic star mass,  $T_{10} = T/10$ ,  $T$  is the orbital period in days,  $R_8 = R_{min}/10^8$  cm,  $R_{min}$  is the minimal distance from the compact object up to which free Keplerian motion is still possible and  $\beta$  is the accretion disk axis inclination angle with respect to the radial direction. For black holes  $R_{min} = 3R_g$ , where  $R_g = 2GM_{bh}/c^2$ .

### 7. Accretion induced collapse and compact objects merging

WD and NS are degenerate configurations, which have upper limit of their mass (the Chandrasekhar and Oppenheimer-Volkov limits correspondingly). The Chandrasekhar limit depends on chemical composition of the white dwarf

$$M_{Ch} = \begin{cases} 1.44M_\odot, & \text{He WD,} \\ 1.40M_\odot, & \text{CO WD,} \\ 1.38M_\odot, & \text{ONeMg WD,} \end{cases} \quad (63)$$

If the mass of WD becomes equal to  $M_{Ch}$ , the WD loses stability and collapses. The collapse is accompanied by the powerful thermonuclear burst observed as a type Ia supernova. Collapses of He and CO WDs leave no remnants (Nomoto & Kondo 1991). The outcome of the collapse of a ONeMg WD is not clear. It can lead to the formation of a neutron star (the accretion induced collapse, AIC). Some papers come to the different conclusion about the result of AICs (see e.g. Garcia-Berro & Iben (1994); Ritossa et al. (1996)). The question about the NS formation during the WD collapse remains undecided. Nevertheless, some NSs could have been formed from AIC WD (van Paradijs 1997). In the ‘‘Scenario Machine’’ code the possibility of NS formation during ONeMg WD is optional.

The merging of two compact objects in a binary WD system (e.g., due to the GW losses) should likely to be similar to AIC. During the merging of two helium WDs, one object with a mass of less than  $M_{Ch}$  (for example,  $0.5M_{\odot} + 0.6M_{\odot} \rightarrow 1.1M_{\odot}$ ) can form. At the same time, if the total mass of the components exceeds  $1.0 - 1.2M_{\odot}$ , a thermonuclear burning can happen. It is likely that the merging of a ONeMg WD with another WD can form a NS.

For the typical NS mass  $\approx 1.4M_{\odot}$ , the binary NS+NS merging event can produce a black hole. Massive ( $\approx 2.8M_{\odot}$ ) neutron star can be formed only if the NS equation of state is very hard and  $M_{OV} \simeq 2.8 - 3.0M_{\odot}$ .

BH+BH merging should produce a rapidly rotating black hole with the mass equal to the total mass of the coalescing binary.

## 8. Additional scenarios of stellar wind from massive stars

### 8.1. Evolutionary scenario B

In the end of 1980s and in the beginning of 1990s the series of new evolutionary tracks were calculated. The authors used new tables of opacities (Rogers & Iglesias 1991; Kurucz 1991), new cross-sections in nuclear reactions (Landre et al. 1990) and new parameters of convection in stars (Stothers & Chin 1991). For stars with  $M < 10M_{\odot}$  those tracks proved to be almost coincident with previous calculations. More massive stars had much stronger stellar winds.

A massive star loses up to 90% of its initial mass in the main-sequence, supergiant, and Wolf-Rayet stages via stellar wind. Therefore, the presupernova mass in this case can be  $\approx 8 - 10M_{\odot}$ , essentially independent of the initial mass of the star (de Jager et al. 1988; Nieuwenhuijzen & de Jager 1990; Schaller et al. 1992).

### 8.2. Evolutionary scenario C

The papers mentioned above were criticised and in 1998 a new version of the evolutionary scenario was developed (Vanbever et al. 1998). The stellar wind loss rates were corrected taking into account empirical data about OB and WR stars. Here we list the main equations of this scenario

(all results concern only with the stars with initial mass  $M_0 > 15M_{\odot}$ ).

$$\log \dot{M} = \begin{cases} 1.67 \log L - 1.55 \log T_{eff} - 8.29, & (\alpha) \\ \log L + \log R - \log M - 7.5, & (\beta) \\ 0.8 \log L - 8.7, & (\gamma) \\ \log L - 10, & (\delta) \end{cases} \quad (64)$$

We assume the next indication in this formula: ( $\alpha$ ), H burning in the core; ( $\beta$ ), giant,  $M_0 \geq 40M_{\odot}$ ; ( $\gamma$ ), giant,  $M_0 < 40M_{\odot}$ ; ( $\delta$ ), Wolf-Rayet star.

Note that in this subsection we used the mass  $M$  is in  $M_{\odot}$ , the luminosity  $L$  is in  $L_{\odot}$  and the radius  $R$  is in  $R_{\odot}$ . With these new calculations, the Webbink diagram described above changed significantly Vanbever et al. (1998).

In this scenario, the total mass loss by a star is calculated using the formula

$$\Delta M = (M - M_{core}), \quad (65)$$

where  $M_{core}$  is the stellar core mass (66). If the maximum mass of the star (usually it is the initial mass of a star, but the mass transfer in binary systems is able to increase its mass above its initial value)  $M_{max} > 15M_{\odot}$ , the mass of the core in the main sequence stage is determined using (66 $\alpha$ ), and in giant and supergiant stages using (66 $\beta$ ). In the Wolf-Rayet star stage (helium star), if  $M_{WR} < 2.5M_{\odot}$  and  $M_{max} \leq 20M_{\odot}$  it is described using (66 $\gamma$ ), if  $M_{WR} \geq 2.5M_{\odot}$  and  $M_{max} \leq 20M_{\odot}$  as (66 $\delta$ ), if  $M_{max} > 20M_{\odot}$  as (66 $\epsilon$ )

$$m_{core} = \begin{cases} 1.62m_{opt}^{0.83} & (\alpha) \\ 10^{-3.051+4.21 \lg m_{opt}-0.93(\lg m_{opt})^2} & (\beta) \\ 0.83m_{WR}^{0.36} & (\gamma) \\ 1.3 + 0.65(m_{WR} - 2.4) & (\delta) \\ m_{core} = 3.03m_{opt}^{0.342}(\epsilon) & (\epsilon) \end{cases} \quad (66)$$

These evolutionary scenarios have some peculiar properties with respect to the classical scenario. One of them is that the strong stellar wind from massive stars leads to a rapid and significant increase of the system's orbit and such stars cannot fill its RL at all.

There are three observational facts that conflict with the strong stellar wind scenarios:

1. A very high  $\dot{M}$  is a problem by itself. The observers calculate this quantity for most of OB and WR stars using the emission measure  $EM \propto \int n_e^2 dl$ . The estimate of  $\dot{M}$  using EM is maximal for homogenous wind. However, there are evidences (see e.g. Cherepashchuk et al. (1984)) that stellar winds of massive stars are strongly “clumpy”. In this case the real  $\dot{M}$  must be 3-5 times less. This note is especially important for the scenario with high stellar wind.
2. Very massive Wolf-Rayet stars do exist. There are at least three double WR+OB systems including very massive WR-stars: CQ Cep  $40M_\odot$ , HD 311884  $48M_\odot$  and HD92740  $77M_\odot$  (Cherepashchuk et al. 1996). Such heavy WR stars are at odds with the assumed high mass loss rate.
3. In the semi-detached binary system RY Sct (W Ser type) the mass of the primary component is  $\approx 35M_\odot$  (Cherepashchuk et al. 1996). This mass is near the limit (Vanbevern et al. 1998) beyond which the star, according to the high mass loss scenario, cannot fill its RL.

### 8.3. Evolutionary Scenario W

The evolutionary scenario W is based on the stellar evolution calculations by Woosley et al. (Woosley et al. (2002), Fig. 16), which represents the relationship between the mass of the relativistic remnant and the initial mass of the star. We included into population-synthesis code two models with W-type stellar winds, which we label Wb and Wc. In models Wb and Wc, the mass-loss rates were computed as in scenario B and scenario C, respectively. The use of these models to calculate the wind rate in a scenario based on Woosley’s diagram (Woosley et al. (2002), Fig. 16) is justified by the fact that scenarios B and C are based on the same numerical expressions for the mass-loss rates from Schaller et al. (1992); Vanbevern et al. (1998); Nieuwenhuijzen & de Jager (1990) that were used by Woosley et al. (2002).

## 9. The “Ecology” of Magnetic Rotators

One of the most important achievements in astrophysics in the end of the 1960s was the realization that in addition to “ordinary” stars, which draw energy from nuclear reactions, there are objects in the Universe whose radiation is caused by a strong gravitational and magnetic field. The well-known examples include neutron stars and white dwarfs. The property that these objects have in common is that their astrophysical manifestations are primarily determined by interaction with the surrounding matter.

In the early 1980s, this approach led to the creation of a complete classification scheme involving various regimes of interaction between neutron stars and their environment, as well as to the first Monte Carlo simulation of the NS evolution (Lipunov 1984). In addition to NSs, this scheme has been shown to be applicable to other types of magnetized rotating stars.

By virtue of the relationship between the gravitational and electromagnetic forces, the NS in various states can manifest itself quite differently from the astronomical point of view. Accordingly, this leads to the corresponding classification of NS types and to the idea of NS evolution as a gradual changing of regimes of interaction with the environment. The nature of the NS itself turns out to be important also when constructing the classification scheme. This indicates that there should be a whole class of quite different objects which have an identical physical nature. To develop the theory describing properties of such objects (in a sense, it should establish “ecological” links between different objects), it proved to be convenient to use symbolic notations elaborated for the particular case of NS. We start this subsection with recollecting the magnetic rotator formalism (mainly according to the paper Lipunov (1987)).

### 9.1. A Gravimagnetic Rotator

We call any gravitationally-bounded object having an angular momentum and intrinsic magnetic field by the term “gravimagnetic rotator” or simply, rotator. In order to specify the intrinsic properties of the rotator, three parameters are sufficient – the mass  $M$ , the total angular momentum  $J = I\omega$  ( $I$  is the moment of inertia and  $\omega$  is the angular velocity), and the magnetic dipole

moment  $\mu$ . Given the rotator radius  $R_0$ , one can express the magnetic field strength at the poles  $B_0$  by using the dipole moment  $B_0 = 2\mu/R_0^3$ . The angle  $\beta$  between the angular momentum  $\mathbf{J}$  and the magnetic dipole moment  $\mu$  can also be of importance:  $\beta = \arccos(J\mu)$ .

## 9.2. The Environment of the Rotator

We assume that the rotator is surrounded by an ideally conductive plasma with a density  $\rho_\infty$  and a sound velocity  $a_\infty$  at a sufficiently far distance from the rotator. The rotator moves relative to the environment with a velocity  $v_\infty$ . Under the action of gravitational attraction, the surrounding matter should fall onto the rotator. A rotator without a magnetic field would capture a stationary flow of matter,  $\dot{M}_c$ , which can be estimated using the Bondi-Hole-Lyttleton formulae (Bondi & Hole 1944; Bondi 1952; McCrea 1953):

$$\dot{M}_c = \delta \frac{(2GM)^2}{(a_\infty^2 + v_\infty^2)^{3/2}} \rho_\infty, \quad (67)$$

where  $\delta$  is a dimensionless factor of the order of unity. When one of the velocities,  $a_\infty$  or  $v_\infty$ , far exceeds the other, the accretion rate is determined by the dominating velocity, and can be written in a convenient form as (55).

In the real astrophysical situation, the parameters of the surrounding matter at distances  $R \gg R_G$  can be taken as conditions at infinity<sup>7</sup>.

As already noted, the matter surrounding a NS or a WD is almost always in the form of a high-temperature plasma with a high conductivity. Such accreting plasma must interact efficiently with the magnetic field of the compact star (Amuel' & Guseinov 1968). Hence, the interaction between the compact star and its surroundings cannot be treated as purely gravitational and therefore the accretion is not a purely gas dynamic process. In general, such interaction should be described by the magneto hydrodynamical equations. This makes the already complicated picture of interaction of the compact star with the surrounding medium even more complex.

The following classification of magnetic rotators is based on the essential characteristics

<sup>7</sup> $R_G = \frac{2GM}{v^2}$ .

of the interaction of the plasma surrounding them with their electromagnetic field. This approach was proposed by Shvartsman (1970) who distinguished three stages of interaction of magnetic rotators: the ejection stage, the propeller stage, which was later rediscovered by Illarionov & Sunyaev (1975) and named as such, and the accretion stage. Using this approach, Shvartsman (1971a) was able to predict the phenomenon of accreting X-ray pulsars in binary systems. New interaction regimes discovered later have led to a general classification of magnetic rotators (Lipunov 1982a, 1984; Kornilov & Lipunov 1983a).

It should be noted that the interaction of the magnetic rotator with the surrounding plasma is not yet understood in detail. However, even the first approximation reveals a multitude of interaction models. To simplify the analysis, we assume the electromagnetic part of the interaction to be independent of the accreting flux parameters, and vice versa.

Henceforth, we shall assume in almost all cases that the intrinsic magnetic field of a rotator is a dipole field (Landau & Lifshiz 1971):

$$B_d = \frac{\mu}{R^3}(1 + 3 \sin^2 \theta)^{1/2}, \quad (68)$$

This is not just a convenient mathematical simplification. We will show that the magnetoplasma interaction takes place at large distances from the surface of the magnetic rotator, where the dipole moment makes the main contribution. Moreover, the collapse of a star into a NS is known to “cleanse” the magnetic field. Indeed, the conservation of magnetic flux leads to a decrease of the ratio of the quadrupole magnetic moment  $q$  to the dipole moment  $\mu$  in direct proportion to the radius of the collapsing star,  $q/\mu \propto R$ .

It should be emphasized, however, that the contribution of the quadrupole component to the field strength at the surface remains unchanged.

The light cylinder radius is the first important characteristic of the rotating magnetic field:

$$R_l = \frac{c}{\omega}, \quad (69)$$

where  $c$  is the speed of light.

A specific property of the field of the rotating magnetic dipole in vacuum is the stationarity of

the field inside the light cylinder and formation of magneto dipole radiation beyond the light cylinder. The luminosity of the magnetic dipole radiation is equal to (Landau & Lifshiz 1971):

$$L_m = \frac{2}{3} \frac{\mu^2 \omega^4}{c^3} \sin^2 \beta = k_t \frac{\mu^2}{R_l^3} \omega, \quad (70)$$

where  $k_t = \frac{2}{3} \sin^2 \beta$ .

This emission exerts a corresponding braking torque

$$\mathbf{K}_m = - \left( \frac{2}{3} \right) \frac{\mu^2 \sin^2 \beta}{c^3} \omega^3 \mathbf{c}_\omega, \quad (71)$$

leading to a spin down of the rotator. Although magnetic dipole radiation from pulsars do not exist, almost all models predict energy loss quantity near this value. At the same time we do not take into account possibly complicated angular dependence of such loss.

### 9.3. The Stopping Radius

Now we consider qualitatively the effect of the electromagnetic field of a magnetic rotator on the accreting plasma. Consider a magnetic rotator with a dipole magnetic moment  $\mu$ , rotational frequency  $\omega$ , and mass  $M$ . At distances  $R \gg R_G$  the surrounding plasma is characterized by the following parameters: density  $\rho_\infty$ , sound velocity  $a_\infty$  and/or velocity  $v_\infty$  relative to the star. The plasma will tend to accrete on to the star under the action of gravitation. The electromagnetic field, however, will obstruct this process, and the accreting matter will come to a stop at a certain distance.

Basically, two different cases can be considered:

- When the interaction takes place beyond the light cylinder,  $R_{stop} > R_l$ . This case first considered by Shvartsman (1970, 1971a). In this case the magnetic rotator generates a relativistic wind consisting of a flux of different kinds of electromagnetic waves and relativistic particles. The form in which the major part of the rotational energy of the star is ejected is not important at this stage. What is important is that both relativistic particles and magnetic dipole radiation will transfer their momentum and hence exert

pressure on the accreting plasma. Indeed, random magnetic fields are always present in the accreting plasma. The Larmor radius of a particle with energy  $\ll 10^{10}$  eV moving in the lowest interstellar magnetic field  $\sim 10^{-6}$  G is much smaller than the characteristic values of radius of interaction, so the relativistic wind will be trapped by the magnetic field of the accreting plasma and thus will transfer its momentum to it.

Thus, a relativistic wind can effectively impede the accretion of matter. A cavern is formed around the magnetic rotator, and the pressure of the ejected wind  $P_m$  at its boundary balances the ram pressure of the accreting plasma  $P_a$ :

$$P_m(R_{stop}) = P_a(R_{stop}), \quad (72)$$

This equality defines a characteristic size of the stopping radius, which we call the Shvartzman radius  $R_{Sh}$ .

- The accreting plasma penetrates the light cylinder  $R_{stop} < R_l$ . The pressure of the accreting plasma is high enough to permit the plasma to enter the light cylinder. Since the magnetic field inside the light cylinder decreases as a dipole field, the magnetic pressure is given by

$$P_m = \frac{B^2}{8\pi} \approx \frac{\mu^2}{8\pi R^6}, \quad (73)$$

Matching this pressure to the ram pressure of the accreting plasma yields the Alfvén radius  $R_A$ .

The magnetic pressure and the pressure of the relativistic wind can be written in the following convenient form:

$$P_m = \begin{cases} \frac{\mu^2}{8\pi R^6}, & R \leq R_l, \\ \frac{L_m}{4\pi R^2 c}, & R > R_l, \end{cases} \quad (74)$$

We introduce a dimensionless factor  $k_t$  such that the power of the ejected wind is

$$L_m = k_t \frac{\mu^2}{R_l^3} \omega, \quad (75)$$

Assuming  $k_t = 1/2$  we get for  $R = R_l$  a continuous function  $P_m = P_m(R)$ .

The accreting pressure of plasma outside the capture radius is nearly constant, and hence gravitation does not affect the medium parameters significantly. In contrast, at distances inside the gravitational capture radius  $R_G$  the matter falls almost freely and exerts pressure on the “wall” equal to the dynamical pressure. For spherically symmetric accretion we obtain

$$P_a = \begin{cases} \frac{\dot{M}v_\infty}{4\pi R_G^2}, & R > R_G, \\ \frac{\dot{M}v_\infty}{4\pi R_G^2} \left(\frac{R_G}{R}\right)^{1/2}, & R \leq R_G, \end{cases} \quad (76)$$

Here we used the continuity equation  $\dot{M}_c = 4\pi R_G^2 \rho_\infty v_\infty$ . When presented in this form, the pressure  $P_a$  is a continuous function of distance.

Summarizing, for the stopping radius we get

$$R_{stop} = \begin{cases} R_a, & R_{stop} \leq R_l, \\ R_{Sh}, & R_{stop} > R_l, \end{cases} \quad (77)$$

The expressions for the Alfvén radius are:

$$R_A = \begin{cases} \left(\frac{2\mu^2 G^2 M^2}{M_c v_\infty^2}\right)^{1/6}, & R_A > R_G, \\ \left(\frac{\mu^2}{2M_c \sqrt{2GM}}\right)^{2/7}, & R_A \leq R_G, \end{cases} \quad (78)$$

and for the Shvartzman radius:

$$R_{Sh} = \left(\frac{8k_t \mu^2 G^2 m^2 \omega^4}{\dot{M}_c v_\infty^5 c^4}\right)^{1/2}, \quad R_{Sh} > R_G, \quad (79)$$

#### 9.4. The Stopping Radius in the Supercritical Case

The estimates presented above for the stopping radius were obtained under the assumption that the energy released during accretion does not exceed the Eddington limit, so we neglected the reverse action of radiation on the accretion flux parameters.

Now, we turn to the situation where one cannot neglect the radiation pressure. Consider this effect after Lipunov (1982b). Suppose that the accretion rate of matter captured by the magnetic rotator is such that the luminosity at the stopping radius exceeds the Eddington limit (see equation 38).

We shall assume, following Shakura & Sunyaev (1973), that the radiation sweeps away exactly that amount of matter which is needed for the accretion luminosity of the remaining flux to be of the order of the Eddington luminosity at any radius:

$$\dot{M}(R) \frac{GM}{R} = L_{edd}, \quad (80)$$

This yields

$$\dot{M}(R) = \dot{M}_c \frac{R}{R_s}, \quad R_s = \frac{\kappa}{4\pi c} \dot{M}_c, \quad (81)$$

where  $R_s$  is a spherization radius (where the accretion luminosity first reaches the Eddington limit), and  $\kappa$  designates the specific opacity of matter. Using the continuity equation, the ram pressure of the accreting plasma is now obtained as another function of the radial distance

$$P_a \approx \rho v^2 \approx \frac{\dot{M}(R)}{4\pi R^2} v = \frac{\dot{M}_c \sqrt{2GM}}{4\pi R_s} R^{-3/2}, \quad R \leq R_s, \quad (82)$$

in contrast to the subcritical regime when  $P_a \propto R^{-5/2}$ . Matching  $P_a$  and  $P_m$  (see the previous section) for the supercritical case gives

$$R_A = \left(\frac{\mu^2 \kappa}{8\pi c \sqrt{2GM_x}}\right)^{2/9}, \quad (83)$$

$$R_{Sh} = \left(\frac{\kappa k_t \mu^2 \omega^4}{4\pi c^5 \sqrt{2GM}}\right)^2, \quad (84)$$

The critical accretion rate  $\dot{M}_{cr}$  is defined by the boundary of the inequality

$$\dot{M}_c \geq \dot{M}_{cr}, \quad (85)$$

and, correspondingly, is

$$\dot{M}_{cr} = \frac{4\pi c}{\kappa} R_{st}. \quad (86)$$

The dependence of the Alfvén radius on the accretion rate is such that the Alfvén radius (beyond the capture radius) slightly decreases with increasing accretion rate as  $\dot{M}^{-1/6}$ , while it decreases below the capture radius as  $\dot{M}^{-2/7}$  and attains its lowest value for the critical accretion rate  $\dot{M}_c > \dot{M}_{cr}$ , beyond which it is independent of the external conditions.

We also note that in the supercritical regime, the pressure of the accreting plasma increases more slowly (as  $R^{-3/2}$ ) when approaching the magnetic rotator than the pressure of the relativistic wind (as  $R^{-2}$ ) ejected by it. This means that in the supercritical case a cavern may exist even below the capture radius.

The estimates presented here, of course, are most suitable for the case of disk accretion. In fact, the supercritical regime seems to emerge most frequently under these conditions. This can be simply understood. Indeed, the accretion rate is proportional to the square of the capture radius  $\dot{M}_c \propto R_G^2$ . At the same time, the angular momentum of the captured matter is also proportional to  $R_G^2$ . Hence, at high accretion rates the formation of the disk looks natural.

### 9.5. The Effect of the Magnetic Field

Apparently, the magnetic field of a star becomes significant only when the stopping radius exceeds the radius of the star,  $R_{st} > R_x$ . We take the Alfvén radius  $R_A$  for  $R_{st}$ , since it is the smallest of the two quantities  $R_A$  and  $R_{Sh}$ . Hence, we can estimate the lowest value of magnetic field of a star which will influence the flow of matter

$$\mu_{min} = \left. \begin{array}{l} \left( \frac{\dot{M}_c v_\infty^5 R_x^6}{4G^2 \dot{M}_x^2} \right)^{1/2}, R_A > R_G, \\ \left( \dot{M}_c \sqrt{GM_x} R_x^{7/2} \right)^{1/2}, R_A \leq R_G \\ \left( \frac{4\pi c \sqrt{2GM_x} R_x^{9/2}}{\kappa} \right), \dot{M}_c > \dot{M}_{cr}, \end{array} \right\} \dot{M}_c \leq \dot{M}_{cr}, \quad (87)$$

The case  $R_A \geq R_G$ ,  $\dot{M}_c \geq \dot{M}_{cr}$  is considered most frequently, and for this case we get the following numerical estimations

$$\mu_{min} = 10^{26} R_6^{7/4} \dot{M}_{17}^{1/2} m_x^{1/4} \text{ G cm}^3, \quad (88)$$

or, equivalently,

$$B_{min} = 10^7 R_6^{5/4} \dot{M}_{17}^{1/2} m_x^{1/4} \text{ G}, \quad (89)$$

Most presently observed NS have magnetic fields  $\sim 10^{12}$  G and dipole moments  $\sim 10^{30}$  G cm<sup>3</sup>, so the magnetic field must necessarily be taken into account when considering interaction of matter with these stars.

### 9.6. The Corotation Radius

The corotation radius is another important characteristic of a magnetic rotator. Suppose that an accreting plasma penetrates the light cylinder and is stopped by the magnetic field at a certain distance  $R_{st}$  given by the balance between the static magnetic field pressure and the plasma pressure. Suppose that the plasma is “frozen” in the rotator’s magnetic field. This field will drag the plasma and force it to rotate rigidly with the angular velocity of the star. The matter will fall on to the stellar surface only if its rotational velocity is smaller than the Keplerian velocity at the given distance  $R_{st}$ :

$$\omega R_{st} < \sqrt{GM_x/R_{st}}, \quad (90)$$

Otherwise, a centrifugal barrier emerges and the rapidly rotating magnetic field impedes the accretion of matter (Shvartsman 1970; Pringle & Rees 1972; Davidson & Ostriker 1973; Lamb 1973; Illarionov & Sunyaev 1975). The latter authors assumed that if  $\omega R_{st} \gg \sqrt{GM_x/R_{st}}$ , the magnetic field throws the plasma back beyond the capture radius. They called this effect the “propeller” regime. In fact, matter may not be shed (Lipunov 1982a), but it is important to note that a stationary accretion is also not possible.

The corotation radius is thus defined as

$$R_c = (GM_x/\omega^2)^{1/3} \sim 2.8 \times 10^8 m_x^{1/3} (P/1s)^{2/3} \text{ cm}, \quad (91)$$

where  $P$  is the rotational period of the star.

If  $R_{st} < R_c$ , rotation influences the accretion insignificantly. Otherwise, a stationary accretion is not possible for  $R_{st} > R_c$ .

### 9.7. Nomenclature

The interaction of a magnetic rotator with the surrounding plasma to a large extent depends on the relation between the four characteristic radii: the stopping radius,  $R_{st}$ , the gravitational capture radius,  $R_G$ , the light cylinder radius,  $R_l$ , and the corotation radius,  $R_c$ . The difference between the

interaction regimes is so significant that the magnetic rotators behave entirely differently in different regimes. Hence, the classification of the interaction regimes may well mean the classification of magnetic rotators. The classification notation and terminology is described below and summarized in Table 1, based on paper by Lipunov (1987).

Naturally, not all possible combinations of the characteristic radii can be realized. For example, the inequality  $R_l > R_c$  is not possible in principle. Furthermore, some combinations require unrealistically large or small parameters of magnetic rotators. Under the same intrinsic and external conditions, the same rotator may gradually pass through several interaction regimes. Such a process will be referred to as the *evolution of a magnetic rotator*.

We describe the classification by considering an idealized scenario of evolution of magnetic rotators. Suppose the parameters  $\rho_\infty$ ,  $v_\infty$  and  $\dot{M}_c$  of the surrounding medium remain unchanged. We shall also assume for a while a constancy of the rotator's magnetic moment  $\mu$ . Let the potential accretion rate  $\dot{M}_c$  at the beginning be not too high, so that the reverse effect of radiation pressure can be neglected,  $\dot{M}_c \leq \dot{M}_{cr}$ . We also assume that the star initially rotates at a high enough speed to provide a powerful relativistic wind.

**Ejectors (E).** We shall call a magnetic rotator an *ejecting star* (or simply an *ejector E*) if the pressure of the electromagnetic radiation and ejected relativistic particles is so high that the surrounding matter is swept away beyond the capture radius or radius of the light cylinder (if  $R_l > R_G$ ).

$$\text{Ejector: } R_{Sh} > \max(R_l, R_G), \quad (92)$$

It follows from here that  $P_m \propto R^{-2}$  while the accretion pressure within the capture radius is  $P_a \propto R^{5/2}$  i.e. increases more rapidly as we approach an accreting star. Consequently, the radius of a stable cavern must exceed the capture radius (Shvartsman 1970).

It is worth noting that the reverse transition from the propeller (P) stage to the ejector (E) stage is non-symmetrical and occurs at a lower period (see below). This means that to switch a pulsar on is more difficult than to turn it off. This is due to the fact that in the case of turning-on of the pulsar the pressures of plasma and relativis-

tic wind must be matched at the surface of the light cylinder, not at the gravitational capture radius. In fact, the reverse transition occurs under the condition of equality of the Alfvén radius to the radius of the light cylinder ( $R_A = R_l$ ).

It should be emphasized that, as mentioned by (Shvartsman 1970), relativistic particles can be formed also at the propeller stage by a rapidly rotating magnetic field (see also Kundt (1990)).

**Propellers (P).** After the ejector stage, the propeller stage sets in under quite general conditions, when accreting matter at the Alfvén surface is hampered by a rapidly rotating magnetic field of the magnetic rotator. In this regime the Alfvén radius is greater than the corotation radius,  $R_A > R_c$ . A finite magnetic viscosity causes the angular momentum to be transferred to the accreting matter so that the rotator spins down. Until now, the propeller stage is one of the poorly investigated phenomena. However, it is clear that sooner or later the magnetic rotator is spin down enough for the rotational effects to be of no importance any longer, and the accretion stage sets in.

**Accretors (A).** In the accretion stage, the stopping radius (Alfvén radius) must be smaller than the corotation radius  $R_A < R_c$ . This is the most thoroughly investigated regime of interaction of magnetic rotators with accreting plasma. Examples of such systems span a wide range of bright observational phenomena from X-ray pulsars, X-ray bursters, low-mass X-ray binaries to most of the cataclysmic variables and X-ray transient sources.

**Georotators (G).** Imagine that the star begins rotating so slowly that it cannot impede the accretion of plasma, i.e. all the conditions mentioned in the previous paragraph are satisfied. However, matter still can not fall on to the rotator's surface if the Alfvén radius is larger than the gravitational capture radius (Illarionov & Sunyaev 1975; Lipunov 1982c). This means that the attractive gravitational force of the star at the Alfvén surface is not significant. A similar situation occurs in the interaction of solar wind with Earth's magnetosphere. The plasma mainly flows around the Earth's magnetosphere and recedes to infinity. This analogy explains the term "georotator" used for this stage. Clearly, a georotator must either have a strong

Table 1: Classification of neutron stars and white dwarfs.

Abbreviation	Type	Characteristic radii relation	Accretion rate	Well known observational appearances
E	Ejector	$R_{st} > R_G$ $R_{st} > R_l$	$\dot{M} \leq \dot{M}_{cr}$	Radio pulsars
P	Propeller	$R_c > R_{st}$ $R_{st} \leq R_G$ $R_{st} \leq R_l$	$\dot{M}_c \leq \dot{M}_{cr}$	?
A	Accretor	$R_{st} \leq R_G$ $R_{st} \leq R_l$	$\dot{M}_c \leq \dot{M}_{cr}$	X-ray pulsars
G	Georotator	$R_G \leq R_{st}$ $R_{st} \leq R_c$	$\dot{M}_c \leq \dot{M}_{cr}$	?
M	Magnetor	$R_{st} > a$ $R_c > a$ ?	$\dot{M}_c \leq \dot{M}_{cr}$	AM Her, polars, soft gamma repeaters, anomalous X-ray pulsars
SE	Super-ejector	$R_{st} > R_l$	$\dot{M}_c > \dot{M}_{cr}$	?
SP	Super-propeller	$R_c < R_{st}$ $R_{st} \leq R_l$	$\dot{M}_c > \dot{M}_{cr}$	?
SA	Super-accretor	$R_{st} \leq R_c$ $R_{st} \leq R_G$	$\dot{M}_c > \dot{M}_{cr}$	?

magnetic field or be embedded in a strongly rarefied medium.

**Magnetors (M).** When a rotator enters a binary system, it may happen that its magnetosphere engulfs the secondary star. Such a regime was considered by Mitrofanov et al. (1977) for WD in close binary systems called polars due to their strongly polarized emission. In the case of NS, magnetors M may be realized only under the extreme condition of very close binaries with no matter within the binary separation.

**Supercritical interaction regimes.** So far, we have assumed that the luminosity at the stopping surface is lower than the Eddington limit. This is fully justified for G and M regimes since gravitation is not important for them. For types E, P, and especially A, however, this is not always true. The critical accretion rate for which the Eddington limit is achieved is

$$\dot{M}_{cr} = 1.5 \times 10^{-6} R_8 M_\odot \text{ yr}^{-1}, \quad (93)$$

where  $R_8 \equiv R_{st}/10^8$  cm is the stopping radius (Schwartzman radius or Alfvén radius, see above).

We stress here that the widely used condition

of supercritical accretion rate

$$\dot{M} \gtrsim 10^{-8} (M/M_\odot) M_\odot \text{ yr}^{-1}$$

is valid *only* for the case of non-magnetic NS, where  $R_{st} \approx 10$  km coincides with the stellar radius. In reality, for a NS with a typical magnetic field of  $10^{11} - 10^{12}$  G, the Alfvén radius reaches  $10^7 - 10^8$  cm, so much higher accretion rates are required for the supercritical accretion to set in. The electromagnetic luminosity released at the NS surface, however, will be restricted by  $L_{edd}$ , and most of the liberated energy may be carried away by neutrinos (Basko & Sunyaev 1975) (see also section about hyper accretion).

Most of the matter in the dynamic model of supercritical accretion forms an outflowing flux covering the magnetic rotator by an opaque shell (Shakura & Sunyaev 1973). The following three additional types are distinguished, depending on the relationship between the characteristic radii: superejector (SE), superpropeller (SP) and super-accretor (SA).

### 9.8. A Universal Diagram for Gravimagnetic Rotators

The classification given above was based on relations between the characteristic radii, i.e. quantities which cannot be observed directly. This drawback can be removed if we note that the light cylinder radius  $R_l$ , Shvartzman radius  $R_{Sh}$  and corotation radius  $R_c$  are functions of the well-observed quantity, rotational period of the magnetor  $p$ . Hence, the above classification can be reformulated in the form of inequalities for the rotational period of a magnetic rotator.

One can introduce two critical periods  $p_E$  and  $p_A$  such that their relationship with period  $p$  of a magnetic rotator specifies the rotator's type:

$$\begin{aligned} p < p_E, & \rightarrow \text{E or SE,} \\ p_E \leq p < p_A, & \rightarrow \text{P or SP,} \\ p > p_A, & \rightarrow \text{A, SA, G or M,} \end{aligned} \quad (94)$$

The values of  $p_E$  and  $p_A$  can be determined from Table 2 which defines the basic nomenclature, and are functions of the parameters  $v_\infty$ ,  $\dot{M}_c$ ,  $\mu$  and  $M_x$ . The parameters  $p$  and  $\mu$  characterize the electromagnetic interaction, while  $\dot{M}_c$  describes the gravitational interaction. Instead of  $\dot{M}_c$  we introduce the potential accretion luminosity  $L$

$$L \equiv \dot{M}_c \frac{GM_x}{R_x}, \quad (95)$$

The physical sense of the potential luminosity is quite clear: the accreting star would be observed to have this luminosity if the matter formally falling on the gravitational capture cross-section were to reach its surface.

Approximate expressions for critical periods (Lipunov 1992) are:

$$p_E = \begin{cases} 0.42v_7^{-1/4} \mu_{30}^{1/2} L_{38}^{-1/4} \text{ s,} & (\alpha) \\ 1.8v_7^{-5/6} m^{1/3} \mu_{30}^{1/3} L_{38}^{-1/6} \text{ s,} & (\beta) \\ 1.4 \cdot 10^{-2} m^{-1/9} \mu_{30}^{4/9} \text{ s,} & (\gamma) \end{cases} \quad (96)$$

We assume the next indication in this formula: ( $\alpha$ ),  $\dot{M}_c \leq \dot{M}_{cr}$ ,  $p \leq p_{GL}$ ; ( $\beta$ ),  $\dot{M}_c \leq \dot{M}_{cr}$ ,  $p > p_{GL}$ ; ( $\gamma$ ),  $\dot{M}_c > \dot{M}_{cr}$ .

$$p_A = \begin{cases} 400v_7^{-5/4} \mu_{30}^{1/2} L_{38}^{-1/4}, & \text{s, } (\alpha) \\ 1.2m^{-5/7} \mu_{30}^{6/7} L_{38}^{-3/7}, & \text{s, } (\beta) \\ 0.17m^{-2/3} \mu_{30}^{2/3}, & \text{s, } (\gamma) \end{cases} \quad (97)$$

We assume the next indication in this formula: ( $\alpha$ ),  $\dot{M}_c \leq \dot{M}_{cr}$  and  $R_A > R_G$ ; ( $\beta$ ),  $\dot{M}_c \leq \dot{M}_{cr}$  and  $R_A \leq R_G$ ; ( $\gamma$ ),  $\dot{M}_c > \dot{M}_{cr}$ .

Here a new critical period  $p_{GL}$  was introduced from the condition  $R_G = R_l$ :

$$p_{GL} = \frac{4\pi GM_x}{v_\infty^2 c} \approx 500m_x v_7^{-2} \text{ s,} \quad (98)$$

Treating the rotator's magnetic dipole moment  $\mu$  and  $M_x$  as parameters, we find that an overwhelming majority of the magnetor's stages can be shown on a "p-L" diagram (Lipunov 1982a). The quantity  $L$  also proves to be convenient because it can be observed directly at the accretion stage.

### 9.9. The Gravimagnetic Parameter

By expecting the expression for the stopping radius in the subcritical regime ( $\dot{M}_c \leq \dot{M}_{cr}$ ) one can note that the magnetic dipole moment  $\mu$  and the accretion rate  $\dot{M}_c$  always appear in the same combination,

$$y = \frac{\dot{M}_c}{\mu^2}, \quad (99)$$

as was noticed by Davies & Pringle (1981). The parameter  $y$  characterizes the ratio between the gravitational and magnetic "properties" of a star and will, therefore, be called the *gravimagnetic parameter*. Two magnetic rotators having quite different magnetic fields, subjected to different external conditions but with identical gravimagnetic parameters, have similar magnetospheres, as long as the accretion rate is quite low ( $\dot{M}_c \leq \dot{M}_{cr}$ ). Otherwise, the flux of matter near the stopping radius no longer depends on the accretion rate at a large distance.

In fact, the number of independent parameters can be further reduced (see e.g. Lipunov (1992)) by introducing the parameter

$$Y = \frac{\dot{M}_c v_\infty}{\mu^2}, \quad (100)$$

Table 2: Parameter of the evolution equation of a magnetic rotators.

Parameter	Regime					
	E, SE	P, SP	A	SA	G	M
$\dot{M}$	0	0	$\dot{M}_c$	$\dot{M}_c(R_A/R_s)$	0	$\dot{M}_c$
$\kappa_t$	$\sim 2/3$	$\lesssim 1/3$	$\sim 1/3$	$\sim 1/3$	$\sim 1/3$	$\sim 1/3$
$R_t$	$R_l$	$R_m$	$R_c$	$R_c$	$R_A$	a

Plotting the rotator’s period  $p$  versus  $Y$ -parameter we can draw a somewhat less obvious but more general classification diagram than the “p-L” diagram discussed above. This permits us to show on a single plot the rotators with key parameters  $\dot{M}_c$ ,  $\mu$  and  $v_\infty$  spanning a very wide range.

In the case of supercritical accretion, another characteristic combination is found in all the expressions:

$$Y_s = \frac{\kappa\mu^2}{v_\infty}, \quad (101)$$

In analog to the subcritical “p-Y” diagram, a supercritical “p- $Y_s$ ” diagram can be drawn.

## 10. Evolution of Magnetic Rotators

The evolution of a magnetic rotator, which determines its observational manifestations, involves the slow changing of the regimes of its interaction with the surrounding medium. Such an approach to the evolution was developed in the 1970s by Shvartsman (1970); Bisnovatyi-Kogan & Komberg (1976); Illarionov & Sunyaev (1975); Shakura (1975); Wickramasinghe & Whelan (1975), Savonije & van den Heuvel (1977) and others. Three stages were mostly considered in these papers: ejector, propeller and accretor. All these stages can be described by a unified evolutionary equation.

### 10.1. The evolution equation

Analysis of the nature of interaction of a magnetized star with the surrounding plasma allows us to write an approximate evolution equation for the angular momentum of a magnetic rotator in the general form (Lipunov 1982a):

$$\frac{dI\omega}{dt} = \dot{M}k_{su} - \kappa_t \frac{\mu^2}{R_t^3}, \quad (102)$$

where  $k_{su}$  is a specific angular momentum applied by the accretion matter to the rotator. This quantity is given by

$$k_{su} = \begin{cases} (GM_x R_d)^{1/2}, & \text{Keplerian disk accretion,} \\ \eta_t \Omega R_G^2, & \text{wind accretion in a binary,} \\ \sim 0, & \text{a single magnetic rotator.} \end{cases} \quad (103)$$

where  $R_d$  is the radius of the inner disk edge,  $\Omega$  is the rotational frequency of the binary system, and  $\eta_t \approx 1/4$  (Illarionov & Sunyaev 1975). The values of dimensionless factor  $\kappa_t$ , characteristic radius  $R_t$  and the accretion rate  $\dot{M}$  in different regimes are presented in Table 2.

The evolution equation (102) is approximate. In practice, the situation with propellers and superpropellers is not yet clear. In Table 2  $R_m$  is the size of a magnetosphere whose value at the propeller stage is not known accurately and which may differ significantly from the standard expressions for the Alfvén radius.

### 10.2. The equilibrium period

The evolution equation presented above indicates that an accreting compact star must endeavor to attain an equilibrium state in which the resultant torque vanishes (Davidson & Ostriker 1973; Lipunov & Shakura 1976). This hypothesis is confirmed by observations of X-ray pulsars.

By equating the right-hand side of equation (103) to zero, we obtain the equilibrium period:

$$\begin{aligned} p_{eq} &\approx 7.8\pi \sqrt{\kappa_t/\epsilon^2} (GM_x)^{-5/7} \eta^{-3/7} \text{ s}, & (\alpha) \\ p_{eq} &= \sqrt{A/B_w} L_{37}^{-1/2} T_{10}^{-1/6} \text{ s}, & (\beta) \end{aligned} \quad (104)$$

where  $A \approx 5 \times 10^{-4} (3\kappa_t) \mu_{30}^2 I_{45}^{-1} m_x^{-1}$  s yr<sup>-1</sup>, and  $B_w \approx 5.2 \times 10^{-6} R_6^2 m_0^{2/3} / (10^{2/3} m_x^2) I_{45}^{-1} \dot{M}_{-6} \eta$  s yr<sup>-1</sup>,  $L_{37} = L/10^{37}$ ,  $T_{10} = T/10$  days; ( $\alpha$ ), disk accretion; ( $\beta$ ), quasi-spherical accretion.

Alternatively:

$$\begin{aligned} p_{eq} &\approx 1.0 L_{37}^{-3/7} \mu_{30}^{6/7} \text{ s, disk,} \\ p_{eq} &= 10 \eta_k^{-1/2} \dot{M}_{-6}^{-1/2} \times \\ &\times (m_0^{2/3} / (10^{2/3} m_x^2))^{-1/2} \times \\ &\times L_{37}^{-1} T_{10}^{-1/6} \mu_{30} \text{ s, stellar wind,} \end{aligned} \quad (105)$$

Let us turn to the case of disk accretion. The above model of the spin-up and spin-down torques possesses an unexpected property. The equilibrium period obtained by setting the torque to zero is connected with the critical period  $p_A$  through a dimensionless factor:

$$p_{eq}(A) = 2^{3/4} \frac{\kappa_t^{1/2}}{\varepsilon^{7/4}} p_A, \quad (106)$$

The parameters  $\kappa_t$  and  $\varepsilon$  must be such that  $p_{eq} > p_A$ . Since  $\kappa_t \approx \varepsilon \approx 1$ , the equilibrium period in the case of disk accretion is close to the critical period,  $p_A$ , separating accretion stage  $A$  and the propeller stage  $P$ . In the case of the supercritical accretion the equilibrium period is determined by formula

(Lipunov 1982b):

$$p_{eq}(SA) \simeq 0.17 \mu_{30}^{2/3} m_x^{-1/9} \text{ s,} \quad (107)$$

### 10.3. Evolutionary Tracks

The evolution of NS in binaries must be studied in conjunction with the evolution of normal stars. This problem was discussed qualitatively by Bisnovatyi-Kogan & Komberg (1976); Savonije & van den Heuvel (1977), Lipunov (1982a) and other. We begin with the qualitative analysis presented in the latter of these paper.

The most convenient method of analysis of NS evolution is using the "p-L" diagram. It should be recalled that  $L$  is just the potential accretion luminosity of the NS. This quantity is equal to the real luminosity only at the accretion stage.

In Figure 1 we show the evolutionary tracks of a NS. As a rule, a NS in a binary is born when the companion star belongs to the main sequence

(loop-like track). During the first  $10^5 - 10^7$  years, the NS is at the ejector stage, and usually it is not seen as a radiopulsar since its pulse radiation is absorbed in the stellar wind of the normal star. The period of the NS increases in accordance with the magnetic dipole losses. After this, the matter penetrates into the light cylinder and the NS passes first into the propeller stage and then into the accretor stage. By this time, the normal star leaves the main sequence and the stellar wind strongly increases. This results in the emergence of a bright X-ray pulsar. The period of the NS stabilizes around its equilibrium value. Finally, the normal star fills the Roche lobe and the accretion rate suddenly increases; the NS moves first to the right and then vertically downward in the "p-L" diagram. In other words, the NS enters the supercritical stage SA (superaccretor) and its spin period tends to a new equilibrium value (see equation (107)).

After the mass exchange, only the helium core of the normal star is left (a WR star in the case of massive stars), the system becomes detached and the NS returns back to the propeller or ejector state. Accretion is still hampered by rapid NS rotation. This is probably the reason underlying the absence of X-ray pulsars in pairs with Wolf-Rayet stars (Lipunov 1982c). Since the helium star evolves on a rather short time-scale ( $\approx 10^5$  yr), the NS does not have time to spindown considerably: after explosion of the normal star, the system can be disrupted leaving the old NS as an ejector, i.e. as a high-velocity radio pulsar.

The "loop-shaped" track discussed above can be written in the form:

- I+E → I+P → II+P → II+A → III+SA → IV+P → E+E (recycled pulsar) → ...
- I+E → I+P → II+A → III+SA → IV+E → (recycled ejector) → IV+P → E+E (recycled pulsar) → ...
- Another version of the evolutionary track of a NS formed in the process of mass exchange within a binary system is:  
III+SE → III+SP → IV+P → E+E → ...

The overall lifetime of a NS in a binary system depends on the lifetime of the normal star and on the parameters of the binary system. However,

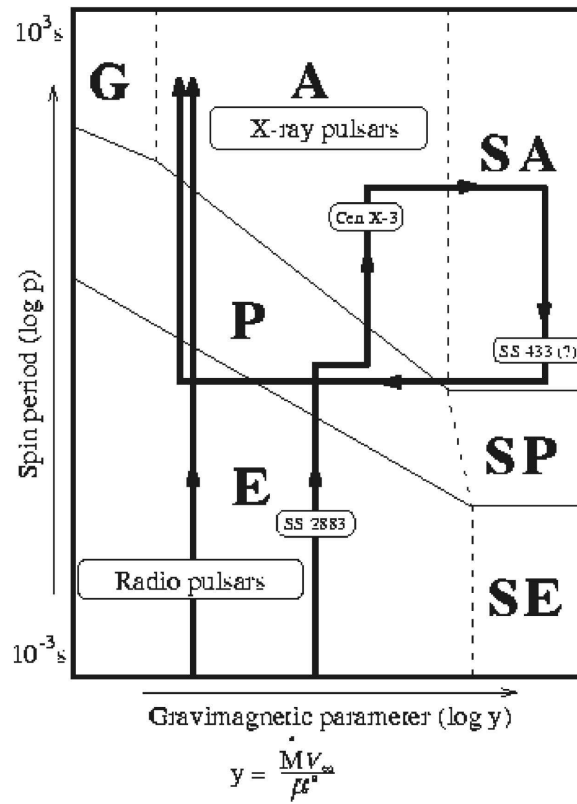


Fig. 1.— Tracks of NS on the period ( $p$ ) - gravimagnetic parameter ( $Y$ ) diagram: track of a single NS (vertical line) and of a NS in a binary system (looped line). For the second track, possible observational appearances of the NS are indicated.

the number of transitions from one stage to another during the time the NS is in the binary is proportional to the magnetic field strength of the NS.

Figure 2 demonstrates the effect of NS magnetic field decay (track (a) with and (b) without magnetic field decay). The first track illustrates the common path which results in the production of a typical millisecond pulsar.

#### 10.4. Evolution of Magnetic Rotators in Non-circular Orbits

So far we have considered evolution of a magnetic rotator related to single rotators or those entering binary system with circular orbits. This approximation was appropriate for the gross analysis of binary evolutionary scenario performed by Kornilov & Lipunov (1983a,b). This approximation is further justified by the fact that the tidal interaction in close binaries leads to orbital circularization in a short time (Hut 1981). However, the more general case of a binary with eccentric orbit must be considered for further analysis. It is especially important because many of the currently observed X-ray pulsars, as well as radio pulsars with massive companions PSR B1259-63 (Johnston et al. 1992) and PSR B0042-73 (Kaspi et al. 1994), are in highly eccentric orbits around massive companions. Previously, such studies have been performed by Gnusareva & Lipunov (1985); Prokhorov (1987).

Orbital eccentricity necessarily emerges after the first supernova explosion and mass expulsion from the binary system. In massive binaries with long orbital periods  $\gtrsim 10$  days, the eccentricity may be well conserved until the second episode of mass exchange (Hut 1981). Here, we concentrate on the evolutionary consequences of eccentricity.

#### 10.5. Mixing types of E-P-A binary systems with non-zero orbital eccentricity

The impact of eccentricity on the observed properties of X-ray pulsars has been considered in many papers (Amnuel' & Guseinov 1971; Shakura & Sunyaev 1973; Pacini & Shapiro 1975; Lipunov & Shakura 1976). The most important consequence of orbital eccentricity for the evolution of rotators can be understood without de-

tailed calculations, and suggests the existence of two different types of binary systems separated by a critical eccentricity,  $e_{cr}$  (Gnusareva & Lipunov 1985).

Consider an ideal situation when a rotator enters a binary system with some eccentricity. The normal star (no matter how) supplies matter to the compact magnetized rotator. We assume that all the parameters of the binary system (binary separation, eccentricity, masses, accretion rate, etc.) are stationary and unchanged. Then a critical eccentricity  $e_{cr}$  appears such that at  $e > e_{cr}$  the rotator is not able to reach the accretion state in principle. Let the rotator be rapid enough initially to be at the ejector (E) state. With other parameters constant, the evolution of such a star is determined only by its spindown. The star will gradually spindown to such a state that when passing close to the periastron where the density of the surrounding matter is higher, the pulsar will “choke” with plasma and pass into the propeller regime. Therefore, for a small part of its life the rotator will be in a mixed EP-state, being in the propeller state at periastron and at the ejector state close to apastron. The subsequent spindown of the rotator leads most probably to the propeller state along the entire orbit. This is due to the fact that the pressure of matter penetrating the light cylinder  $R_l$  increases faster than that caused by relativistic wind and radiation, as first noted by Shvartsman (1971a). So it proves to be much harder for the rotator to pass from the P state to the E state than from E to P state (see the following section).

The rotator will spindown ultimately to some period,  $p_A$ , at which accretion will be possible during the periastron passage. Accretion, in contrast, will lead to a spin-up of the rotator, so that it reaches some average equilibrium state characterized by an equilibrium period  $p_{eq}$  defined by the balance of accelerating and decelerating torques averaged over the orbital period. If the eccentricity was zero, the rotator would be in the accretion state all the time. By increasing the eccentricity and keeping the periastron separation between the stars unchanged, we increase the contribution of the decelerating torque over the orbital period and thus decrease  $p_{eq}$ . At some ultimate large enough eccentricity  $e_{cr}$  the equilibrium period will be less than the critical period  $p_A$  permitting the transi-

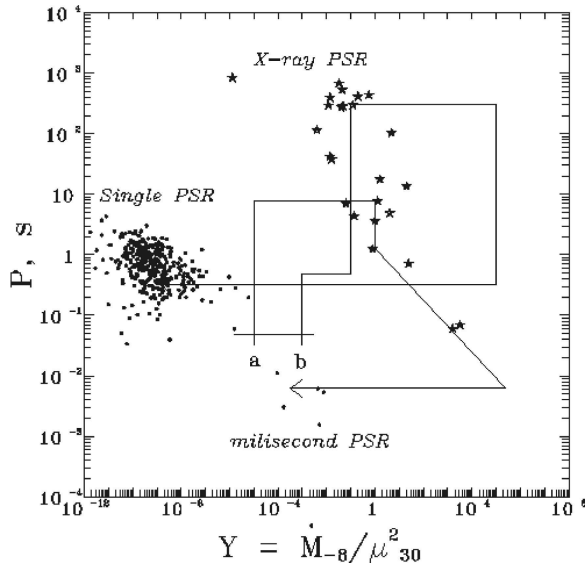


Fig. 2.— The period-gravimagnetic parameter diagram for NS in binary systems. (a) with NS magnetic field decay (the oblique part of the track corresponds to “movement” of the accreting NS along the so-called “spin-up” line), (b) a typical track of a NS without field decay in a massive binary system.

tion from the propeller state to the accretion state at apastron to occur. The rotational torque applied to the rotator, averaged over orbital period, vanishes, and in this sense the equilibrium state is achieved, but the rotator periodically passes from the propeller state to the accretion state.

Thus, X-ray pulsars with unreachable full-orbit accretion state must exist. This means that from the observational point of view such binaries will be observed as transient X-ray sources with stationary parameters for the normal component.

Typically, the evolutionary track of a rotator in an eccentric binary is

- $E \rightarrow PE \rightarrow P \rightarrow AP$ ,  $e > e_{cr}$
- $E \rightarrow PE \rightarrow P \rightarrow AP \rightarrow A$ ,  $e < e_{cr}$

this may be the principal formation channel of transient X-ray sources.

### 10.6. Ejector-propeller hysteresis

As mentioned earlier, the transition of the rotator from the ejector state to the propeller state is not symmetrical. Here we consider this effect in more detail. In terms of our approach, we must study the dependence of  $R_{st}$  on  $\dot{M}_c$ . To find  $R_{st}$ ,

we must match the ram pressure of the accreting plasma with that caused by the relativistic wind or by the magnetosphere of the rotator. This dependence  $R_{st}(\dot{M}_c)$  will be substantially different for rapidly ( $R_l < R_G$ ) and slowly ( $R_l > R_G$ ) rotating stars (see Figure 3). One can see that in the case of a fast rotator, an interval of  $\dot{M}_c$  appears where three different values of  $R_{st}$  are possible, the upper value  $R_1$  corresponding to the ejector state and the bottom value  $R_3$  to the propeller state; the intermediate value  $R_2$  is unstable. This means that the rotator’s state is not determined solely by the value of  $\dot{M}_c$ , but also depends on previous behavior of this value.

Now consider a periodic changing of  $\dot{M}_c$  caused, for example, by the rotator’s motion along an eccentric orbit, and large enough for the rotator to transit from the ejector state to the propeller state and vice versa. Initially, the rotator is in the ejector state. By approaching the normal star, the accretion rate  $\dot{M}_c$  increases and reaches a critical value  $\dot{M}_{EP}$ , where the equilibrium points  $R_1$  (stable point corresponding to the ejector state) and  $R_2$  (unstable) approach  $R_G$  (upper kink), where they merge (see Figure 2). After that only one equilibrium point remains in the system, the stopping radius  $R_{st}$  jumps from  $\approx R_G$  down to

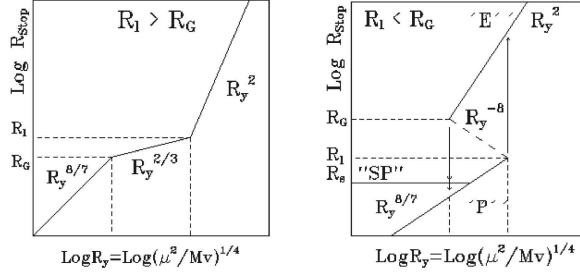


Fig. 3.— Dependence of the stopping radius  $R_{st}$  on the modified gravimagnetic radius  $R_y$  for two possible relations between the light cylinder radius  $R_l$  and the gravitation capture radius  $R_G$ :  $R_l > R_G$  (left-hand panel) and  $R_l < R_G$  (right-hand panel; here the ejector-propeller hysteresis becomes possible).

$R_3 < R_l$ , and the rotator changes to the propeller state.

As  $\dot{M}_c$  decreases further along the orbit and reaches the critical value  $\dot{M}_{EP}$  once again, the reverse transition from propeller to ejector does not occur. The transition only occurs when  $\dot{M}_c$  reaches another critical value,  $\dot{M}_{PE} < \dot{M}_{EP}$ , where the unstable point  $R_2$  meets the stable propeller point  $R_3$ , and the stopping radius  $R_{st}$  jumps from  $\sim R_l$  up to  $R_1 > R_G$ . It should be noted that for fast enough rotators, a situation is possible when the step down from the ejector state occurs in such a manner that the stopping radius  $R_{st} < R_c$  and the rotator passes directly to the accretion state. The reverse transition always passes through the propeller stage:  $A \rightarrow P \rightarrow E$ . In principle, transitions from the ejector state to supercritical states SP or SA are also possible (Prokhorov 1987). In the case of slow rotators ( $R_l > R_B$ ), the “E-P” hysteresis is not possible, and transitions between these states are symmetrical.

### 10.7. E-P transitions for different orbits

Orbital motion of the rotator around the normal companion in an eccentric binary draws a horizontal line on the “p-Y” diagram, with the beginning at a point corresponding to  $\dot{M}_c(a_p)$ , and the end at a point corresponding to  $\dot{M}_c(a_a)$  (here  $a_p$  and  $a_a$  are the periastron and apastron distances, respectively). The length of this segment is determined by the eccentricity. Since  $Y \propto \dot{M}_c$ , the rotator moves along this segment from left to right and back as it revolves from the apastron to the periastron. At each successive orbital period, this line slowly drifts up to larger periods. The evolu-

tion of this system is thus determined by the order the critical lines on the diagram are crossed by this “line”. It is seen from the “p-Y” diagram that the regions with and without hysteresis are separated by a certain value of the parameter  $Y = Y_k$ . Since  $Y \propto \dot{M}_c \propto 1/r^2$ , four different situations are possible depending on the relationship of the binary orbital separation  $a$  with critical value  $a_{cr}$ , corresponding to  $Y_k$  (see e.g. Lipunov (1992); Lipunov et al. (1996b)).

1.  $a_p > a_{cr}$ . In this case no hysteresis occurs and transitions E–P and the reverse take place in symmetrical points of the orbit. The rotator passes the following sequence of stages:  $E \rightarrow EP \rightarrow P \rightarrow \dots$  Here EP means a mixed state of the rotator at which it is in the ejector state during one part of the orbit, and in the propeller state during the rest of the orbital cycle.
2.  $a_a > a_{cr} > a_p$ . In this case, the hysteresis occurs at the beginning of the mixed EP-state (state  $EP_h$ ), but as the rotator slows down the hysteresis gradually decays and disappears. E-P transition for this system is:  $E \rightarrow EP_h \rightarrow EP \rightarrow P \rightarrow \dots$
3.  $a_a < a_{cr}$ . The hysteresis is possible in principle, but the shape of the transition depends on the eccentricity. Suppose a pulsar has spun down so much that the first transition from the ejector to the propeller occurred at the periastron. If the eccentricity were small  $e < e_{cr}$ , (do not confuse this  $e_{cr}$  with the critical eccentricity introduced in the previous section) the reverse transition to the

ejector state would not occur even at the apastron, and the evolutionary path would be  $E \rightarrow P \rightarrow \dots$

4. If  $e > e_{cr}$ , the track is  $E \rightarrow EP_h \rightarrow P \rightarrow \dots$ . It should be noted that just after the first EP transition (as well as before the last), the system spends a finite time in the E and P states at every revolution.

The value of  $e_{cr}$  can be expressed through the orbital parameters as

$$e_{cr} \simeq \frac{a_{cr}^{1/7} - a_a^{1/7}}{a_{cr}^{1/7} + a_a^{1/7}}, \quad (108)$$

To conclude, we note that the hysteresis during the ejector-propeller transition may be possible for single radio pulsars also. For example, when the pulsar moves through a dense cloud of interstellar plasma, the pulses can be absorbed. The radio pulsar turns on again when it comes out from the cloud. The hysteresis amplitude for single pulsars can be high enough because of small relative velocities of the interstellar gas and the pulsar, so that  $R_G \gg R_l$ .

## 11. Summary

The ‘‘Scenario Machine’’ is the numerical code for theoretical investigations of statistical properties of binary stars, i.e. this is population synthesis code (Lipunov et al. 1996b). It includes the evolution of normal stars and the evolution of their compact remnants. This is especially important for studies of the neutron stars (Lipunov 1992). We always include the most important observational discoveries and theoretical estimations into our code.

## REFERENCES

- Abt H.A., 1983, Annual review of astronomy and astrophysics, v. 21, p. 343
- Allen C.W., 1973, University of London, Athlone Press, 3rd ed.
- Amnuel’ P.R., Guseinov O.H., 1968, Izv. Akad. Nauk Az. SSR, 3, 70
- Amnuel’ P.R., Guseinov O.Kh., 1971, Soviet Astronomy, v. 15, p. 218
- Basko M.M., Sunyaev R.A., 1975, A&A, 42, 311
- Bisnovatyi-Kogan G.S., Komberg B.V., 1976, Soviet Astronomy, v. 19, p. 279
- Boersma J., 1961, Bulletin of the Astronomical Institutes of the Netherlands, v. 15, p. 291
- Bogomazov A.I., Abubekerev M.K., Lipunov V.M., Cherepashchuk A.M., 2005, Astron. Reports, 49, 295
- Bondi H., 1952, MNRAS, 112, 195
- Bondi H., Hole F., 1944, MNRAS, 104, 273
- Chanmugam G., 19992, Annual review of astronomy and astrophysics, v. 30, p. 143
- Cherepashchuk A.M., Khaliullin Kh., Eaton J.A., 1984, ApJ, v. 281, p. 774
- Cherepashchuk A.M., Katysheva N.A., Khurzina T.S., Shugarov S.Yu., 1996, Highly Evolved Close Binary Stars: Catalog, Gordon & Breach Publ., The Netherlands
- Chevalier R.A., 1993, ApJ, 411, L33
- Davidson K., Ostriker J.P., 1973, ApJ, v. 179, pp. 585
- Davies R.E., Pringle J.E., 1981, MNRAS, 196, 209
- Delgado A.J., Thomas H.-C., 1981, A&A, v. 96, p. 142
- Eggleton P.P., 1983, ApJ, v. 268, p. 368
- Garcia-Berro E., Iben I., 1994, ApJ, v. 434, p. 306
- Gnusareva V.S., Lipunov V.M., 1985, Soviet Astronomy, v.29, p. 645
- Hut P., 1981, A&A, 99, 126
- Iben I. Jr., Tutukov A. V., 1985, ApJ, 58, 661-710
- Iben Icko Jr., Tutukov Alexander V., 1987, ApJ, 313, 727-742
- Illarionov A.F., Sunyaev R.A., 1975, A&A, v. 39, p. 185
- van den Heuvel E.P.J., 1983, Accretion-driven stellar X-ray sources, p. 303

- van den Heuvel E.P.J., Heise J., 1972, *Nature Physical Science*, v. 239, p. 67
- de Jager C., 1980, *The Brightest Stars*, Reidel, Dordrecht
- de Jager C., Nieuwenhuijzen H., van der Hucht K.A., 1988, *A&AS*, v. 72, p. 259
- Johnston S., Manchester R.N., Lyne A.G., et al., 1992, *ApJ*, 387, L37
- Joss P.C., Rappaport S., 1983, *ApJL*, 270, 73
- Kalogera V., Webbink R.F., 1998, *ApJ*, 493, 351
- Karpov S.V., and Lipunov V.M., 2001, *Astron. Letters*, 27, 10, 645-647
- Kaspi V.M., Johnston S., Bell J.F., et al., 1994, *ApJ*, 423, L43
- Kawaler S.D., 1988, *ApJ*, 333, 236
- Kippenhahn R., Weigert A., 1967, *Zeitschrift fur Astrophysik*, v. 65, p. 251
- Kolb U., King A.R., Ritter H., 1998, *MNRAS*, 298, L29
- Kornilov V.G., Lipunov V.M., 1983, *Soviet Astronomy*, v. 27, p. 163
- Kornilov V.G., Lipunov V.M., 1983, *Soviet Astronomy*, v. 27, p. 334
- Karpov S.V., and Lipunov V.M., *Astron. Letters*, 2001, 27, 10, 645-647
- Krajcheva Z.T., Popova E.I., Tutukov A.V., Yungelson L.R., 1981, *SvA Lett.*, 7, 269
- Kudritzki B.P., Reimers D., 1978, *A&A*, 70, 227
- Kundt W., 1990, In *Neutron Stars and their Birth Events*, ed. W.Kundt, Kluwer Academic Publishers, Dordrecht, p. 1
- Kurucz R.L., *New Opacity Calculations*, 1991, In *Stellar Atmospheres: Beyond Classical Models*, Proceedings of the Advanced Research Workshop, Trieste, Italy, Dordrecht, D. Reidel Publishing Co., p.441
- Lamb F.K., Pathick C.J., Pines D., 1973, *ApJ*, 184, 271
- Lamers H. J. G. L. M., 1981, *ApJ*, 1, 245, 593-608
- Landau L.D., Lifshiz E.M., 1971, *Classical Theory of Fields*, Addison-Wesley, Reading, Massachusetts and Pergamon Press, London
- Landre V., Prantzos N., Aguer P., Bogaert G., Lefebvre A., Thibaud J.P., 1990, *A&A*, v. 240, p. 85
- Lipunov V.M., 1982a, *Ap&SS*, 82, 343
- Lipunov V.M., 1982b, *SvA*, 26, 54
- Lipunov V.M., 1982c, *SvAL*, 8, 194
- Lipunov V.M., 1982, *Soviet Astronomy*, 26, 537
- Lipunov V.M., 1984, *Advances in Space Research*, v. 3., no. 10-12, p. 323
- Lipunov V.M., 1987, *Ap&SS*, 132, 1
- Lipunov V.M., 1992, *Astrophysics of Neutron Stars*, Springer-Verlag, Berlin - Heidelberg - New York, Astronomy and Astrophysics Library, 322
- Lipunov V.M., 2006, *IAU proceedings, Populations of High Energy Sources in Galaxies Proceedings of the 230th Symposium of the International Astronomical Union*, Edited by E.J.A. Meurs, G. Fabbiano, Cambridge University Press, 2006, p. 391 in Q.Z., van Paradijs J., van den Heuvel E.P.J., 2000, *A&A*, 368, 1021
- Lipunov V.M., Ozernoy L.M., Popov S.B., Postnov K.A., Prokhorov M.E., 1996a, *ApJ*, 466, 234
- Lipunov V.M., Postnov K.A., 1988, *Ap&SS*, v. 145, no. 1, p. 1-45.
- Lipunov V.M., Postnov K.A., Prokhorov M.E., 1996b, ed. Sunyaev R.A., *The Scenario Machine: Binary Star Population Synthesis*, Astrophysics and Space Physics Reviews, vol. 9, Harwood academic publishers
- Lipunov V.M., Postnov K.A., Prokhorov M.E., 1996, *A&A*, 310, 489
- Lipunov V.M., Postnov K.A., Prokhorov M.E., 1997, *MNRAS*, 288, 245
- Lipunov V.M., Shakura N.I., 1976, *Soviet Astronomy Letters*, v. 2, no. 4, p. 133

- Lyne A.G. et al., 2004, *Science*, v. 303, pp. 1153-1157
- Mardling R.A., 1995a, *ApJ*, 450, 722
- Mardling R.A., 1995b, *ApJ*, 450, 732
- McCrea W.H., 1953, *MNRAS*, 113, 162
- Mestel L., 1952, 136, 583
- Mitrofanov I.G., Pavlov G.G., Gnedin Yu.N., 1977, *Astron. Tsirk.*, 948, 5
- Nieuwenhuijzen H., de Jager C., 1990, *A&A*, v. 231, p. 134
- Nomoto K., Kondo Y., 1991, *ApJ*, v. 367, p. L19
- Pacini F., Shapiro S.L., 1975, *Nature*, 255, 618
- Paczyn'ski B., *Annual Review of Astronomy and Astrophysics*, 1971, v. 9, p. 183
- Paczynski B., 1976, *IAU Proceedings of the Symposium no. 73, Structure and Evolution of Close Binary Systems*, Edited by P. Eggleton, S. Mitton, and J. Whelan, Dordrecht, D. Reidel Publishing Co., p. 75
- Paczynski B., Sienkiewicz R., 1983, *ApJ*, 268, 825
- van Paradijs J., van den Heuvel E.P.J., Kouveliotou C., Fishman G.J., Finger M.H., Lewin W.H.G., *A&A*, v. 317, p. L9
- Peters P.C., *Phys. Rev.*, 136, 1224
- Peters P.C., Mathews J., 1963, *Phys. Rev.*, 131, 435
- Pols O.R., Marinus M., 1994, *A&A*, 288, 475
- Press W.H., Teukolsky S.A., 1977, *ApJ*, 213, 183
- Pringle J.E., Rees M.J., 1972, *A&A*, 21, 1
- Prokhorov M.E., 1987, *Astron Tsirc.*, 1502, 1
- Rappaport S., Joss P.C., Webbink R.F., 1982, *ApJ*, v. 254, p. 616
- Ritossa C., Garcia-Berro E., Iben I., 1996, *ApJ*, v. 460, p. 489
- Rogers F.J., Iglesias C.A., 1991, *Bulletin of the American Astronomical Society*, v. 23, p. 1382
- Savonije G.J., van den Heuvel E.P.J., 1977, *ApJ*, 214, L19
- Schaller G., Schaerer D., Meynet G., Maeder A., 1992, *A&AS*, v. 96, p. 269
- Shakura N.I., 1975, *Soviet Astronomy Letters*, v. 1, no. 6, p. 223
- Shakura N.I., Sunyaev R.A., 1973, *A&A*, 24, 337
- Shvartsman V.F., *Soviet Astronomy*, v. 14, p. 527
- Shvartsman V.G., *Soviet Astronomy*, v. 14, p. 662
- Shvartsman V.F., 1971, *Soviet Astronomy*, v. 15, p. 342
- Skumanich A., 1972, *ApJ*, v. 171, p. 565
- Stothers R.B., Chin C.-W., 1991, *ApJ*, v. 381, p. L67
- Thorsett S.E., Chakrabarty D., 1999, *ApJ*, 512, 288
- Tout C.A., Pringle J.E., 1992, *MNRAS*, 256, 269
- Trimble V., 1983, v. 303, p. 137
- Tutukov A., Yungelson L., 1973, *Nauchnye Informatsii*, v. 27, p. 70
- Vanbeveren D., de Donder E., van Bever J., van Rensbergen W., de Loore C., 1998, *New Astronomy*, v. 3, p. 443
- Van Bever J., Vanbeveren D., 2000, *A&A*, 358, 462
- van den Heuvel E.P.J., in Shore S.N., Livio M., van den Heuvel E.P.J., 1994, *Interacting Binaries*, Springer-Verlag, p. 103
- Varshavskii, V. I., Tutukov, A. V., 1975, *SvA*, 19, 142
- Verbunt F., 1984, *MNRAS*, 209, 227
- Verbunt F., Zwaan C., 1983, *A&A*, v. 100, p. L7
- Webbink R.F., 1979, *Proceedings of the Fourth Annual Workshop on Novae, Dwarf Novae and Other Cataclysmic Variables*, Rochester N.Y., University of Rochester, p. 426

- Webbink R.F., 1985, Stellar evolution and binaries, in *Interacting Binary Stars*, Ed. Pringle J.E. and Wade R.A., Cambridge Astrophysics Series, Cambridge University Press, p.39
- Wickramasinghe D.T., Whelan J.A.J., 1975, *Nature*, v. 258, p. 502
- Weisberg J.M., Taylor J.H., 2003, proceedings of "Radio Pulsars," Chania, Crete, August, 2002, ASP. Conf. Series, 2003, Edited by M. Bailes, D.J. Nice, S.E. Thorsett
- Woolley S.E., Heger A., Weaver T.A., 2002, *Rev. Mod. Phys.*, v. 74, p. 1015
- Wex N., Kalogera V., Kramer M., 2000, *ApJ*, 528, 401
- Zangrilli L., Tout C.A., Bianchini A., 1997, *MNRAS*, 289, 59
- Zahn J.-P., 1975, *A&A*, 41, 329
- Zahn J.-P., 1989, *A&A*, 220, 112
- Zahn J.-P., Bouchet L., 1989, *A&A*, 223, 112
- Zeldovich Ya.B., Ivanova L.N., Nadezhin D.K., 1972, *Soviet Astronomy*, 16, 209